2012

Robust Load Disturbance Torque Estimation for a Permanent Magnet DC Motor Drive System

Danny Grignion
University of Windsor

Robust Load Disturbance Torque Estimation for a Permanent Magnet DC Motor Drive System

By

Danny Grignion

A Thesis

Submitted to the Faculty of Graduate Studies

through Electrical and Computer Engineering

In Partial Fulfillment of the Requirements for

the Degree of Master of Applied Science at the

University of Windsor

Windsor, Ontario, Canada

2012

Robust Load Disturbance Torque Estimation for a Permanent Magnet DC Motor Drive System

by

Danny Grignion

APPROVED BY:

_____

Dr. B. Minaker
Department of Mechanical, Automotive & Materials Engineering

_____

Dr. S. Chowdhury
Department of Electrical & Computer Engineering

_____

Dr. X. Chen, Co-Advisor
Department of Electrical & Computer Engineering

_____

Dr. N. Kar, Co-Advisor
Department of Electrical & Computer Engineering

_____

Dr. M. Mirhassani, Chair of Defense
Department of Electrical & Computer Engineering

May 8, 2012

DECLARATION OF CO-AUTHORSHIP / PREVIOUS PUBLICATION

I. Co-Authorship Declaration

I hereby declare that this thesis incorporates material that is the result of joint research undertaken in collaboration with Huijie Qian under the supervision of Dr. X. Chen. In all cases, the key ideas, primary contributions, experimental designs, data analysis and interpretation, were performed by the author, and the contribution of the co-author was primarily through the provision of verification of mathematical assumptions and calculations and aid in the acquisition of experimental results.

I am aware of the University of Windsor Senate Policy on Authorship and I certify that I have properly acknowledged the contribution of other researchers to my thesis, and have obtained written permission from each of the co-author(s) to include the above material(s) in my thesis.

I certify that, with the above qualification, this thesis, and the research to which it refers, is the product of my own work.

II. Declaration of Previous Publication

This thesis includes three original papers that have been previously published/submitted for publication in peer reviewed journals, as follows:

Thesis Chapter	Publication title/full citation	Publication status*
Chapter 1,2,3,5	*"Robust Load Disturbance Torque Estimation for a DC Motor Drive System"; 2012 ROCOND Conference, Aalborg, Denmark*	*Accepted*
Chapter 1,2,3,5	*"Improved Load Disturbance Torque Estimation for a DC Motor Drive System"; 2012 IECON Conference, Montréal, Canada*	*Submitted*
Chapter 1,2,3,5	*"Load Disturbance Torque Estimation for a DC Motor Drive System with Robustness Consideration"; IEEE Transactions on Industrial Electronics*	*Submitted*

I certify that I have obtained a written permission from the copyright owner(s) to include the above published material(s) in my thesis. I certify that the above material describes work completed during my registration as graduate student at the University of Windsor.

I declare that, to the best of my knowledge, my thesis does not infringe upon anyone's copyright nor violate any proprietary rights and that any ideas, techniques, quotations, or any other material from the work of other people included in my thesis, published or otherwise, are fully acknowledged in accordance with the standard referencing practices. Furthermore, to the extent that I have included copyrighted material that surpasses the bounds of fair dealing within the meaning of the Canada Copyright Act, I certify that I have obtained a written permission from the copyright owner(s) to include such material(s) in my thesis.

I declare that this is a true copy of my thesis, including any final revisions, as approved by my thesis committee and the Graduate Studies office, and that this thesis has not been submitted for a higher degree to any other University or Institution.

ABSTRACT

Direct current motors are an integral part of many systems. An important factor in the design of these systems is the disturbance torque on the motor's shaft. This disturbance torque can negatively affect the performance of the motor and the overall system. Knowledge of the disturbance can aid in compensating for these negative effects, which enhances the robustness of the system to changes in the load. Estimation has become a feasible means of acquiring the value of such a disturbance. Various methods for the design of a robust disturbance torque estimator are presented here. The designs are robust in the sense that the estimation is insensitive to the presence of model uncertainties and/or noise. The estimators are designed to estimate both constant and non-constant, low-frequency disturbance torques. The designs are tested using a permanent magnet DC motor. An in-line torque sensor is used for validation.

DEDICATION

I dedicate this thesis to all of my family and friends for their continuous encouragement, love and support throughout my graduate studies.

ACKNOWLEDGEMENTS

I would like to express my sincere gratitude and appreciation to Dr. Xiang Chen and Dr. Narayan Kar, my co-supervisors, for accepting me as one of their graduate students, and for their support and guidance throughout this research.

I would also like to express my gratitude and appreciation to Dr. Sazzadur Chowdhury and Dr. Bruce Minaker for their valuable comments and suggestions throughout the evaluation of this thesis and seminar.

This research was supported in part by the Ontario Research Fund, Green Auto Powertrain and NSERC Network Centre of Excellence – AUTO21.

I am very grateful to the University of Windsor for the support of my graduate studies over these two years.

Lastly, I would like to thank all of my fellow graduate students, in particular my lab partner Huijie Qian, and my family and friends for their encouragement and support throughout my time spent as a graduate student.

TABLE OF CONTENTS

LIST OF TABLES

LIST OF FIGURES

LIST OF ABBREVIATIONS

ARE	Algebraic Riccati Equation
BLDC	Brushless DC Motor
DC	Direct Current
IP	Internet Protocol
LAN	Local Area Network
LCF	Left Coprime Factorization
MUT	Motor Under Test
ODE	Ordinary Differential Equation
PMDC	Permanent Magnet DC Motor
PWM	Pulse Width Modulation
RC	Resistor-Capacitor
RSE	Referenced Single Ended
RT	Real-Time
SI	International System of Units (Système international d'unités)
TCP/IP	Transmission Control Protocol/Internet Protocol

NOMENCLATURE

Δ	Variation
ω_m	Motor speed
τ_d	Disturbance torque
τ_E	Electrical time constant
τ_L	Load torque
τ_M	Mechanical time constant
τ_m	Motor torque
τ_s	Measured torque from in-line torque sensor
B_m	Motor viscous friction coefficient
e_a	Back electromotive force
G	Instrumentation amplifier gain
i_a	Armature current
$i_{a_{noise}}$	Measurement noise
J_m	Motor inertial coefficient
K_t	Mechanical constant
K_v	Electrical constant
L_a	Armature inductance
N_E	Encoder pulses counted in the fixed time interval
P_R	Pulses per revolution
R_a	Armature resistance
R_k	Known resistance
R_s	Current shunt resistance
T_i	Fixed time interval

V_{brush} Brush noise

v_c Test motor controller analog input voltage

v_{cdyno} Dyno motor controller analog input voltage

v_d Disturbance voltage

v_{dyno} Dyno motor voltage

v_o Instrumentation amplifier output voltage

v_s In-line torque sensor output voltage

v_t Armature voltage

CHAPTER 1: INTRODUCTION

Direct current (DC) motors are rugged, reliable, cost-effective and easy to use electromechanical machines. This flexibility is what has allowed the DC motor to become commonplace in today's society with numerous applications including automotive, robotics, mechatronics and model railroading to name a few. Modern automobiles contain a myriad of DC motors that control not only various aspects of the vehicle's performance, but that also provide extra luxury and comfort for the driver and passengers. Some examples include electronic throttle control, electric power steering, regenerative braking, sunroof, power locks, power seats and power windows. With all of these applications for the DC motor, it is no surprise that research into not only the design of the motor, but also into the control of the motor is of great importance.

Many factors can affect the performance of a DC motor. Loading conditions and operating temperatures play particularly important roles in these situations. For example, a change in the motor's loading conditions will present itself as a disturbance torque acting on the motor's shaft and will cause the motor's speed and armature current to change. Knowledge of this disturbance torque can be used by the motor's control system in order to properly mitigate its effects.

Also, over time with extended periods of rigorous use, the motor will heat up causing a change in armature resistance. Therefore, it is important when developing a model, estimation strategy or control strategy, to include possible variations in the motor's parameters as uncertainties and to minimize the impact of these uncertainties on the strategies being employed, i.e., to make the strategies robust to such uncertainties.

This thesis will explore different methods to robustly estimate the disturbance torque in a DC motor drive system.

1.1 Disturbance Torque Estimation

Due to the difficulty and cost of direct measurement, estimation has become a popular method of measuring the quantity of the disturbance torque acting on a DC motor's shaft. This estimation may then be used to compensate for the disturbance torque acting on the shaft, thus improving the system's robustness to external torques and load changes. A well designed estimation scheme can also be used to reduce the cost of the overall system as it can be used to estimate other quantities and thus eliminate the need to use high-priced sensors to measure such quantities.

Three disturbance torque estimation schemes are presented in [1]. All of the schemes use a Luenberger observer, see [2]-[5], as a basis for the estimator designs. In order to accomplish this, the plant model is expanded to incorporate the disturbance torque. This expansion is performed in two ways. The first expansion treats the disturbance torque as an unknown input. The second expansion treats the disturbance torque as a state variable. This second method was used successfully in [6] and [7]. There is a restriction placed on the design of this type of estimator in that the disturbance torque acting on the plant is assumed to be constant and only performance for constant disturbance torques is shown. It is not guaranteed that a non-constant disturbance torque can be estimated.

However, none of these schemes incorporate the presence of model uncertainties into the design of the estimator. A disturbance torque estimator that makes use of an observer design that also takes these uncertainties into account would serve not only to provide a good estimation, but also to make the estimation robust to variations in the parameters of the plant. Two such observers that can be used for this purpose are the $\mathcal{H}_\infty$ filter discussed in [8]-[10], and the $\mathcal{H}_\infty$ Gaussian filter presented in

[11] and [12]. These observers are designed to provide a robust estimate of the states of a system in the presence of model uncertainties, and noise in the case of the $\mathcal{H}_\infty$ Gaussian filter. This is achieved through the solution of one, or a set of algebraic Riccati equations (ARE).

All of these designs are conducted in the time-domain using state-space representations of the system model. The flexibility of state observer based designs and the fact that the disturbance torque can be easily related to the state variables of a DC motor provide motivation for using such a design methodology. However it should be noted that a state observer based design is not the only method available to estimate a disturbance. For other designs see [13]-[16].

1.2 Conflicting Requirements

It can be shown that the error dynamics of the DC motor drive system are not only affected by model uncertainties, but also by the disturbance acting on the system, and that the disturbance torque estimation is proportional to the error in estimation of the motor's armature current. This raises an interesting question as to how an observer design can be conducted that both maximizes the sensitivity of the error to the disturbance, while minimizing or constraining the sensitivity of the error to model uncertainties. A good filter design will make a trade-off between these two conflicting requirements. In order to facilitate such a design, two measures are required. One measure is needed in order to properly gauge the sensitivity to uncertainty. This can be easily achieved using the $\mathcal{H}_\infty$ norm. The second measure is needed in order to properly gauge the sensitivity to a disturbance.

The $\mathcal{H}_-$ index can be used for such a purpose. This index can be used to achieve the desired sensitivity to a disturbance by maximizing the $\mathcal{H}_-$ index of the transfer

function from disturbance to error. A mix of these two measures would thus provide a means for achieving such a filter design. One such design is the multi-objective $\mathcal{H}_-/\mathcal{H}_\infty$ filter, presented in [17]-[23], that has been used for fault-detection. In this case the observer was designed to generate a residual signal whose sensitivity was maximized with respect to faults in the system and minimized with respect to disturbances acting on the system.

In the sense of disturbance torque estimation, this design approach can be used in such a way as to relate the disturbance torque to the residual signal and maximize the signal's sensitivity with respect to the disturbance while minimizing its sensitivity with respect to model uncertainties.

1.3 Thesis Outline

Three disturbance torque estimator designs will be developed in this thesis. In particular, an $\mathcal{H}_\infty$ filter, an $\mathcal{H}_\infty$ Gaussian filter and a multi-objective $\mathcal{H}_-/\mathcal{H}_\infty$ filter will be used as a basis for the estimator designs.

Chapter 2 will provide definitions of various norms used in the observer designs. A theoretical background of a generic observer, an $\mathcal{H}_\infty$ filter, an $\mathcal{H}_\infty$ Gaussian filter and an $\mathcal{H}_-/\mathcal{H}_\infty$ filter will also be provided along with a model of the DC motor drive system used to design the estimators.

Chapter 3 discusses the design of the disturbance torque estimators, defines performance criteria for the estimators and develops appropriate combinations of model uncertainties that are to be used for testing the robustness of the disturbance torque estimation.

Chapter 4 details the methods used to determine the parameters of the DC motor that is used to test the disturbance torque estimator designs. The hardware and software used to test the estimators is also detailed.

Chapter 5 presents the parameters used to determine the observer gains as well as the calculated observer gains. Test results of the disturbance torque estimators are also presented accordingly.

Chapter 6 concludes this thesis and provides some recommendations for future work in this area of research.

CHAPTER 2: PRELIMINARY THEORY

2.1 Notations

The following notation is used throughout this thesis. Matrices and vectors are represented using bold lettering. ˆ denotes an estimated state variable and ˙ denotes a derivative with respect to time. If $\boldsymbol{A}$ is a matrix then $\boldsymbol{A^T}$ and $\boldsymbol{A}^*$ denote its transpose and conjugate transpose respectively. $\boldsymbol{I}$ and $\boldsymbol{0}$ denote an identity matrix of appropriate dimensions and a zero matrix of appropriate dimensions respectively. $\bar{\sigma}(\boldsymbol{A})$ and $\underline{\sigma}(\boldsymbol{A})$ denote the largest and smallest singular values of $\boldsymbol{A}$ respectively.

Let $\boldsymbol{G}(s)$ be a proper, real, rational transfer matrix. A state space realization of $\boldsymbol{G}(s)$ is [24]

$$\boldsymbol{G}(s) = \left[\begin{array}{c|c} \boldsymbol{A} & \boldsymbol{B} \\ \hline \boldsymbol{C} & \boldsymbol{D} \end{array}\right] = \boldsymbol{C}(s\boldsymbol{I} - \boldsymbol{A})^{-\mathbf{1}}\boldsymbol{B} + \boldsymbol{D}.$$

A left coprime factorization (LCF), [21], of $\boldsymbol{G}(s)$ is a factorization $\boldsymbol{G}(s) = \boldsymbol{M}^{-\mathbf{1}}(s)\boldsymbol{N}(s)$ where $\boldsymbol{M}(s)$ and $\boldsymbol{N}(s)$ are left-coprime over $\mathcal{RH}_\infty$ and $\mathcal{RH}_\infty$ is the space of all proper and real rational stable matrix transfer functions. Let the state space realization of $\boldsymbol{G}(s)$ above be detectable and let $\boldsymbol{L}$ be a matrix with appropriate dimensions such that $\boldsymbol{A} + \boldsymbol{LC}$ is stable. Then an LCF of $\boldsymbol{G}(s)$ is given by

$$[\boldsymbol{M}(s) \quad \boldsymbol{N}(s)] = \left[\begin{array}{c|cc} \boldsymbol{A}+\boldsymbol{LC} & \boldsymbol{L} & \boldsymbol{B}+\boldsymbol{LD} \\ \hline \boldsymbol{C} & \boldsymbol{I} & \boldsymbol{D} \end{array}\right].$$

2.2 Norm Definitions

The following definitions are used throughout this thesis (see [8]-[12] and [17]-[24]). For $\boldsymbol{G}(s) \in \mathcal{RH}_2$ where $\mathcal{RH}_2$ is the space of all strictly proper and real rational stable matrix transfer functions, the $\mathcal{H}_2$ norm of $\boldsymbol{G}(s)$ is defined as

$$\|\boldsymbol{G}(s)\|_2 = \sqrt{\frac{1}{2\pi}\int_{-\infty}^{\infty} \text{trace}[\boldsymbol{G}^*(j\omega)\boldsymbol{G}(j\omega)]d\omega}.$$

For $\boldsymbol{G}(s) \in \mathcal{RH}_\infty$ the $\mathcal{H}_\infty$ norm of $\boldsymbol{G}(s)$ is defined as

$$\|\boldsymbol{G}(s)\|_\infty = \sup_{\omega\in\mathcal{R}} \bar{\sigma}(\boldsymbol{G}(j\omega)).$$

Similarly the $\mathcal{H}_-$ index of $\boldsymbol{G}(s)$ over all frequencies is defined as

$$\|\boldsymbol{G}(s)\|_-^{[\infty]} = \inf_{\omega\in\mathcal{R}} \underline{\sigma}(\boldsymbol{G}(j\omega)).$$

The $\mathcal{H}_-$ index of $\boldsymbol{G}(s)$ over a finite frequency range $[\omega_1, \omega_2]$ is defined as

$$\|\boldsymbol{G}(s)\|_-^{[\omega_1,\omega_2]} = \inf_{\omega\in[\omega_1,\omega_2]} \underline{\sigma}(\boldsymbol{G}(j\omega)).$$

The $\mathcal{H}_-$ index of $\boldsymbol{G}(s)$ at zero frequency is defined as

$$\|\boldsymbol{G}(s)\|_-^{[0]} = \underline{\sigma}(\boldsymbol{G}(0)).$$

If no superscript is added to the $\mathcal{H}_-$ symbol, such as $\|\boldsymbol{G}(s)\|_-$, then it represents all possible $\mathcal{H}_-$ definitions.

2.3 Generic Observer Model

Any nominal, linear, time-invariant, continuous-time system can be represented by a state space model in the following form:

$$\begin{aligned} \dot{\boldsymbol{x}} &= \boldsymbol{A}\boldsymbol{x} + \boldsymbol{B}\boldsymbol{u} \\ \boldsymbol{y} &= \boldsymbol{C}\boldsymbol{x} + \boldsymbol{D}\boldsymbol{u} \end{aligned} \tag{2-1}$$

where $\boldsymbol{x}$, $\dot{\boldsymbol{x}}$, $\boldsymbol{y}$ and $\boldsymbol{u}$ are vectors that represent the system states, the derivatives with respect to time of the system states, the measurement outputs of the system and the control input of the system respectively, and $\boldsymbol{A}$, $\boldsymbol{B}$, $\boldsymbol{C}$ and $\boldsymbol{D}$ are matrices that are known as the system, input, output and feedthrough matrices respectively.

Assuming that the pair $(\boldsymbol{A}, \boldsymbol{C})$ is observable, i.e. that the observability matrix

$$\boldsymbol{\mathcal{O}} = \begin{bmatrix} \boldsymbol{C} \\ \boldsymbol{CA} \\ \vdots \\ \boldsymbol{CA}^{n-1} \end{bmatrix}$$

where n is the number of state variables, has full column rank, the following observer model can be used for estimation of the system states:

$$\begin{aligned} \dot{\hat{\boldsymbol{x}}} &= \boldsymbol{A}\hat{\boldsymbol{x}} + \boldsymbol{Bu} + \boldsymbol{L}(\boldsymbol{y} - \hat{\boldsymbol{y}}) \\ \hat{\boldsymbol{y}} &= \boldsymbol{C}\hat{\boldsymbol{x}} + \boldsymbol{Du} \end{aligned} \tag{2-2}$$

where $\boldsymbol{L}$ represents the gain of the observer that is to be designed. A general layout of a system with an observer is shown in *Figure 2.1*.

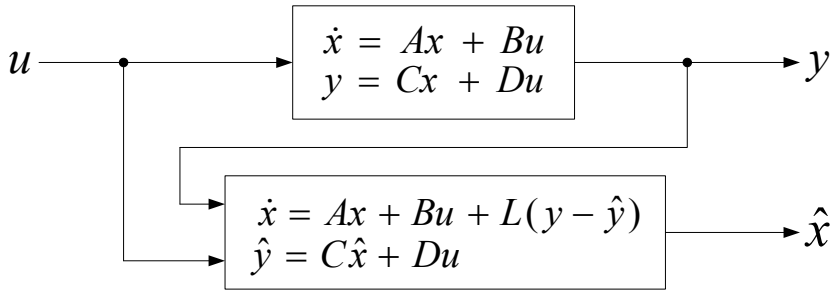

Figure 2.1 General layout of a system with an observer.

The gain $\boldsymbol{L}$ can be chosen using different methods that are geared towards different performance criteria. Note that the state model of the system used to derive the particular observer gain is altered accordingly also based on the desired performance criteria.

2.4 $\mathcal{H}_\infty$ Filter

No physical system is ever ideal. As such, ideal models of these systems are never accurate representations of the physical world. Uncertainties are present in any physical system and must be accounted for in any model that is used for design. These uncertainties could be due to parameters that are either unknown, change over long and extended periods of time, vary due to heating and other temperature effects, or are tolerance values in which the nominal system parameters exist.

The $\mathcal{H}_\infty$ filter, [8]-[10], takes into consideration these various parameter and model uncertainties. This filter is designed to estimate the system states in the presence of uncertainties. The state space model of the system used to calculate the observer gain is in the following form:

$$\begin{aligned} \dot{\boldsymbol{x}} &= \boldsymbol{Ax} + \boldsymbol{Bu} + \boldsymbol{B_1 w} \\ \boldsymbol{y} &= \boldsymbol{Cx} + \boldsymbol{D_{21} w} \\ \boldsymbol{z} &= \boldsymbol{C_1 x} + \boldsymbol{D_{11} w} \end{aligned} \tag{2-3}$$

where $\boldsymbol{B_1}$ is a weighting matrix for the model uncertainties, $\boldsymbol{D_{21}}$ and $\boldsymbol{D_{11}}$ are weighting matrices for the measurement and output uncertainties respectively, $\boldsymbol{w}$ is a vector of uncertainties, $\boldsymbol{C_1}$ is a matrix that allows us to define the desired outputs of the system and $\boldsymbol{z}$ is a vector of the desired outputs of the system.

Using an observer in the form of (2-2) and defining $\boldsymbol{e_x} = \boldsymbol{x} - \hat{\boldsymbol{x}}$ to be the estimation error, the error dynamics of this observer can be calculated as

$$\dot{\boldsymbol{e}}_{\boldsymbol{x}} = \dot{\boldsymbol{x}} - \dot{\hat{\boldsymbol{x}}} = (\boldsymbol{A} - \boldsymbol{LC})\boldsymbol{e_x} + (\boldsymbol{B_1} - \boldsymbol{LD_{21}}) \tag{2-4}$$

where $\dot{\boldsymbol{e}}_{\boldsymbol{x}}$ represents the derivative with respect to time of the estimation error. Reformulating the problem as shown in *Figure 2.2*, an objective used to calculate the value of $\boldsymbol{L}$ for this observer can be defined.

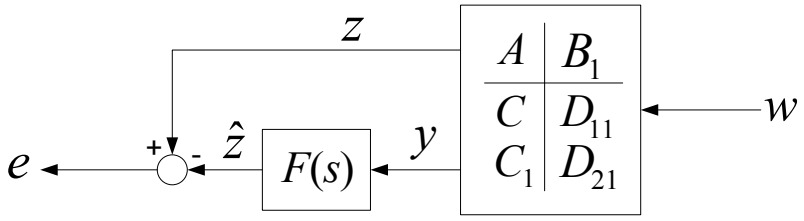

Figure 2.2 $\mathcal{H}_\infty$ estimation problem.

Given a $\gamma > 0$, find a causal filter $\boldsymbol{F}(\boldsymbol{s}) \in \mathcal{RH}_\infty$ if it exists such that:

$$\left\| \boldsymbol{T}_{\boldsymbol{e_x w}} \right\|_\infty = \sup_{\omega \in \mathcal{L}_2[0,\infty)} \frac{\|\boldsymbol{e_x}\|_2^2}{\|\boldsymbol{w}\|_2^2} < \gamma^2 \tag{2-5}$$

where $\mathcal{L}_2[0,\infty)$ is the space of all time domain square integrable functions with functions zero for $t < 0$. Assuming that $\boldsymbol{D_{11}} = \boldsymbol{D_{21}} = \boldsymbol{0}$, this can be achieved by solving the following ARE:

$$\boldsymbol{AP} + \boldsymbol{PA^T} + \boldsymbol{P}\left(\gamma^{-2}\boldsymbol{C_1^T C_1} - \boldsymbol{C^T C}\right)\boldsymbol{P} + \boldsymbol{B_1 B_1^T} = \boldsymbol{0} \tag{2-6}$$

which yields a gain of

$$\boldsymbol{L} = \boldsymbol{PC^T}. \tag{2-7}$$

Note that γ is a positive constant that represents the limit of uncertainty that may be tolerated by the filter.

2.5 $\mathcal{H}_\infty$ Gaussian Filter

Uncertainties are not the only factors that plague physical systems. Noise is another factor that can also have detrimental effects. It can affect not only the measurements obtained through sensors (measurement noise) but can also affect the system itself (process noise). Good filter designs will not only factor in uncertainties, but will also factor in noise.

The $\mathcal{H}_\infty$ Gaussian filter, [11] and [12], not only takes uncertainties and noise into consideration, but also makes a trade-off between the two according to the desired performance specifications. It is designed to estimate the system states in the presence of both model uncertainties and white noise. The state space model of the system used to calculate the observer gain is in the following form:

$$\begin{aligned} \dot{\boldsymbol{x}} &= \boldsymbol{Ax} + \boldsymbol{Bu} + \boldsymbol{B_0 w_0} + \boldsymbol{B_1 w} \\ \boldsymbol{y} &= \boldsymbol{Cx} + \boldsymbol{D_{20} w_0} \\ \boldsymbol{z_0} &= \boldsymbol{C_0 x} \\ \boldsymbol{z} &= \boldsymbol{C_1 x} \end{aligned} \tag{2-8}$$

where $\boldsymbol{B_1}$ is a weighting matrix for the model uncertainties, $\boldsymbol{B_0}$ and $\boldsymbol{D_{20}}$ are input and feedthrough matrices for the process and measurement noises respectively, $\boldsymbol{C_0}$ and $\boldsymbol{C_1}$ are matrices that allow us to define the desired outputs of the system, $\boldsymbol{z_0}$ and $\boldsymbol{z}$ are

vectors of the desired outputs of the system, $\boldsymbol{w}$ is a vector of uncertainties and $\boldsymbol{w_0}$ is a vector of white noises acting on the system. Note that white noise is assumed to satisfy the following conditions:

$$E\{\boldsymbol{w_0}(\boldsymbol{t})\} = \boldsymbol{0}$$
$$E\{\boldsymbol{w_0}(\boldsymbol{t})\boldsymbol{w_0^T}(\boldsymbol{t})\} = \boldsymbol{I}\delta(t-\tau)$$

where $E\{\cdot\}$ is the expectation operator.

Using an observer in the form of (2-2) and defining $\boldsymbol{e_x} = \boldsymbol{x} - \hat{\boldsymbol{x}}$ to be the estimation error, the error dynamics of this observer can be calculated as

$$\dot{\boldsymbol{e}}_{\boldsymbol{x}} = \dot{\boldsymbol{x}} - \dot{\hat{\boldsymbol{x}}} = (\boldsymbol{A} - \boldsymbol{LC})\boldsymbol{e_x} + (\boldsymbol{B_1} - \boldsymbol{LD_{21}}) + \boldsymbol{B_1 w} \tag{2-9}$$

where $\dot{\boldsymbol{e}}_{\boldsymbol{x}}$ represents the derivative with respect to time of the estimation error. Reformulating the problem as shown in *Figure 2.3*, an objective used to calculate the value of $\boldsymbol{L}$ for this observer can be defined.

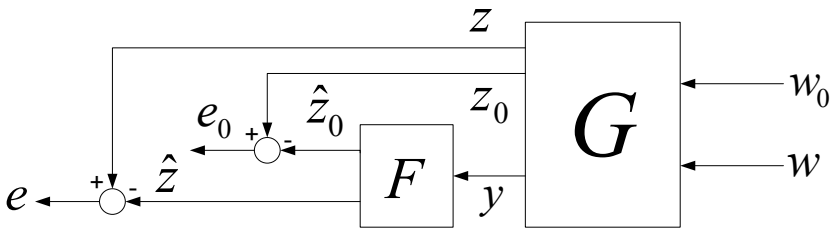

Figure 2.3 $\mathcal{H}_\infty$ Gaussian estimation problem.

Given a $\gamma > 0$, define the following cost functionals:

$$J_1(\boldsymbol{F}, \boldsymbol{w}(\boldsymbol{t}), \boldsymbol{w_0}(\boldsymbol{t})) = \lim_{T\to\infty} \frac{1}{T}\int_0^T E\{\gamma^2 \|\boldsymbol{w}(\boldsymbol{t})\|^2 - \|\boldsymbol{e}(\boldsymbol{t})\|^2\}dt \tag{2-10}$$

$$J_2(\boldsymbol{F}, \boldsymbol{w}(\boldsymbol{t}), \boldsymbol{w_0}(\boldsymbol{t})) = \lim_{T\to\infty} \frac{1}{T}\int_0^T E\{\|\boldsymbol{e_0}(\boldsymbol{t})\|^2\}dt \tag{2-11}$$

Note that $\boldsymbol{F}(\boldsymbol{s})$ must be stable. Therefore we say that $\boldsymbol{F}$ is an admissible filter if $\boldsymbol{F}(\boldsymbol{s}) \in \mathcal{RH}_\infty$.

Find and admissible filter $\boldsymbol{F}_*$ of the form

$$\begin{aligned}\dot{\hat{\boldsymbol{x}}} &= \boldsymbol{A}\hat{\boldsymbol{x}} + \boldsymbol{L}(\boldsymbol{y} - \hat{\boldsymbol{y}}) = (\boldsymbol{A} - \boldsymbol{LC})\hat{\boldsymbol{x}} + \boldsymbol{Ly};\ \ \boldsymbol{x}(0) = \boldsymbol{0} \\ \hat{\boldsymbol{z}}_{\boldsymbol{0}} &= \boldsymbol{C}_{\boldsymbol{0}}\hat{\boldsymbol{x}} \\ \hat{\boldsymbol{z}} &= \boldsymbol{C}_{\boldsymbol{1}}\hat{\boldsymbol{x}}\end{aligned} \tag{2-12}$$

and a worst disturbance signal $\boldsymbol{w}_*(\boldsymbol{t})$ such that

$$J_1\big(\boldsymbol{F}_*, \boldsymbol{w}_*(\boldsymbol{t}), \boldsymbol{w}_{\boldsymbol{0}}(\boldsymbol{t})\big) \le J_1\big(\boldsymbol{F}_*, \boldsymbol{w}(\boldsymbol{t}), \boldsymbol{w}_{\boldsymbol{0}}(\boldsymbol{t})\big)$$

$$J_2\big(\boldsymbol{F}_*, \boldsymbol{w}_*(\boldsymbol{t}), \boldsymbol{w}_{\boldsymbol{0}}(\boldsymbol{t})\big) \le J_2\big(\boldsymbol{F}_*, \boldsymbol{w}(\boldsymbol{t}), \boldsymbol{w}_{\boldsymbol{0}}(\boldsymbol{t})\big)$$

hold for all $\boldsymbol{F} \in \mathcal{P}$ where $\mathcal{P}$ is the space of all stationary signals with bounded power. This can be achieved by solving the following coupled ARE's:

$$\begin{aligned}&\big(\boldsymbol{A} - \boldsymbol{P_2C^TR_0^{-1}C} - \boldsymbol{B_0D_{20}^TR_0^{-1}C}\big)^{\boldsymbol{T}}\boldsymbol{P_1} + \boldsymbol{P_1}\big(\boldsymbol{A} - \boldsymbol{P_2C^TR_0^{-1}C} - \boldsymbol{B_0D_{20}^TR_0^{-1}C}\big) \\ &+\gamma^{-2}\boldsymbol{P_1B_1B_1^TP_1} + \boldsymbol{C_1^TC_1} = \boldsymbol{0}\end{aligned} \tag{2-13}$$

$$\begin{aligned}&\big(\boldsymbol{A} - \boldsymbol{B_0D_{20}^TR_0^{-1}C} + \gamma^{-2}\boldsymbol{B_1B_1^TP_1}\big)\boldsymbol{P_2} + \boldsymbol{P_2}(\boldsymbol{A} - \boldsymbol{B_0D_{20}^TR_0^{-1}C} + \gamma^{-2}\boldsymbol{B_1B_1^TP_1})^{\boldsymbol{T}} \\ &-\boldsymbol{P_2C^TR_0^{-1}CP_2} + \boldsymbol{B_0}\big(\boldsymbol{I} - \boldsymbol{D_{20}^TR_0^{-1}D_{20}}\big)\boldsymbol{B_0^T} = \boldsymbol{0}\end{aligned} \tag{2-14}$$

where $\boldsymbol{R_0} = \boldsymbol{D_{20}D_{20}^T}$. This yields a gain of

$$\boldsymbol{L} = (\boldsymbol{P_2C^T} + \boldsymbol{B_0D_{20}^T})\boldsymbol{R_0^{-1}}. \tag{2-15}$$

Note that γ is a positive constant that the designer can vary so as to fulfill the desired performance specifications. As $\gamma \to \infty$, the performance of the filter towards white noise improves, whereas as $\gamma \to 0$, the performance of the filter towards model uncertainty improves.

2.6 $\mathcal{H}_-/\mathcal{H}_\infty$ Filter

In certain situations, it is desirable to amplify of the sensitivity of a parameter or input that affects the system while simultaneously minimizing the sensitivity of another. For example, in fault detection it is desirable to amplify the sensitivity of a residual signal to a fault while minimizing the sensitivity of the residual signal to a disturbance. In the case of disturbance torque estimation, it is desirable to amplify the sensitivity of a

residual signal to an external disturbance while minimizing the sensitivity of the residual signal to model uncertainties.

The $\mathcal{H}_-/\mathcal{H}_\infty$ filter, [17]-[23], can achieve such a desired performance. It is designed to maximize the sensitivity of the estimation to one parameter or input and making the estimation robust against another. For the purposes of this thesis, the state space model of the system used to calculate the observer gain is in the following form:

$$\begin{aligned} \dot{\boldsymbol{x}} &= \boldsymbol{A}\boldsymbol{x} + \boldsymbol{B}\boldsymbol{u} + \boldsymbol{B_d}\boldsymbol{w_d} + \boldsymbol{B_1}\boldsymbol{w} \\ \boldsymbol{y} &= \boldsymbol{C}\boldsymbol{x} + \boldsymbol{D}\boldsymbol{u} + \boldsymbol{D_d}\boldsymbol{w_d} + \boldsymbol{D_{21}}\boldsymbol{w} \end{aligned} \tag{2-16}$$

where $\boldsymbol{B_d}$ and $\boldsymbol{D_d}$ are input and feedthrough matrices for the disturbances respectively, $\boldsymbol{B_1}$ and $\boldsymbol{D_{21}}$ are weighting matrices for the model uncertainties and output uncertainties respectively, $\boldsymbol{w_d}$ is a vector of external disturbances, and $\boldsymbol{w}$ is a vector of uncertainties.

By taking the Laplace transform of (2-16) we get

$$\boldsymbol{y} = \boldsymbol{G_u}(s)\boldsymbol{u} + \boldsymbol{G_1}(s)\boldsymbol{w} + \boldsymbol{G_d}(s)\boldsymbol{w_d} \tag{2-17}$$

where $\boldsymbol{G_u}(s)$, $\boldsymbol{G_1}(s)$ and $\boldsymbol{G_d}(s)$ are the transfer matrices from input to output, uncertainty to output and disturbance to output respectively, whose state space realizations are

$$[\boldsymbol{G_u}(s) \quad \boldsymbol{G_1}(s) \quad \boldsymbol{G_d}(s)] = \left[\begin{array}{c|ccc} \boldsymbol{A} & \boldsymbol{B} & \boldsymbol{B_1} & \boldsymbol{B_d} \\ \hline \boldsymbol{C} & \boldsymbol{D} & \boldsymbol{D_{21}} & \boldsymbol{D_d} \end{array}\right]. \tag{2-18}$$

An LCF of (2-18) can be written as

$$[\boldsymbol{G_u}(s) \quad \boldsymbol{G_1}(s) \quad \boldsymbol{G_d}(s)] = \boldsymbol{M^{-1}}(s)[\boldsymbol{N_u}(s) \quad \boldsymbol{N_1}(s) \quad \boldsymbol{N_d}(s)] \tag{2-19}$$

where

$$\begin{aligned} &[\boldsymbol{G_u}(s) \quad \boldsymbol{G_1}(s) \quad \boldsymbol{G_d}(s)] \\ &\qquad = \left[\begin{array}{cc|ccc} \boldsymbol{A}+\boldsymbol{LC} & \boldsymbol{L} & \boldsymbol{B}+\boldsymbol{LD} & \boldsymbol{B_1}+\boldsymbol{LD_{21}} & \boldsymbol{B_d}+\boldsymbol{LD_D} \\ \hline \boldsymbol{C} & \boldsymbol{I} & \boldsymbol{D} & \boldsymbol{D_{21}} & \boldsymbol{D_d} \end{array}\right] \end{aligned} \tag{2-20}$$

and $\boldsymbol{L}$ is a matrix such that $\boldsymbol{A}+\boldsymbol{LC}$ is stable.

It can be shown that the filter can take the following general form [21]:

$$\boldsymbol{r} = \boldsymbol{Q}(s)(\boldsymbol{M}(s)\boldsymbol{y} - \boldsymbol{N_u}(s)\boldsymbol{u}) = \boldsymbol{Q}(s)[\boldsymbol{M}(s) \quad -\boldsymbol{N_u}(s)]\begin{bmatrix}\boldsymbol{y}\\ \boldsymbol{u}\end{bmatrix} \tag{2-21}$$

where $\boldsymbol{r}$ is known as the residual vector and $\boldsymbol{Q}(s)$ is a stable transfer matrix to be designed. By replacing $\boldsymbol{y}$ in (2-21) with the right-hand side of (2-17) and (2-19) we get

$$\boldsymbol{r} = \boldsymbol{Q}(s)[\boldsymbol{N_1}(s) \quad \boldsymbol{N_d}(s)] \begin{bmatrix} \boldsymbol{w} \\ \boldsymbol{w_d} \end{bmatrix} = \boldsymbol{Q}(s)\boldsymbol{N_1}(s)\boldsymbol{w} + \boldsymbol{Q}(s)\boldsymbol{N_d}(s)\boldsymbol{w_d}. \tag{2-22}$$

Thus the transfer matrices from uncertainty to residual and disturbance to residual can be written as

$$\boldsymbol{G_{rw}} = \boldsymbol{Q}(s)\boldsymbol{N_1}(s), \qquad \boldsymbol{G_{rd}} = \boldsymbol{Q}(s)\boldsymbol{N_d}(s). \tag{2-23}$$

A block diagram of the system is shown in *Figure 2.4*. From this, an objective can be defined that can be used to design an appropriate $\boldsymbol{Q}(s)$.

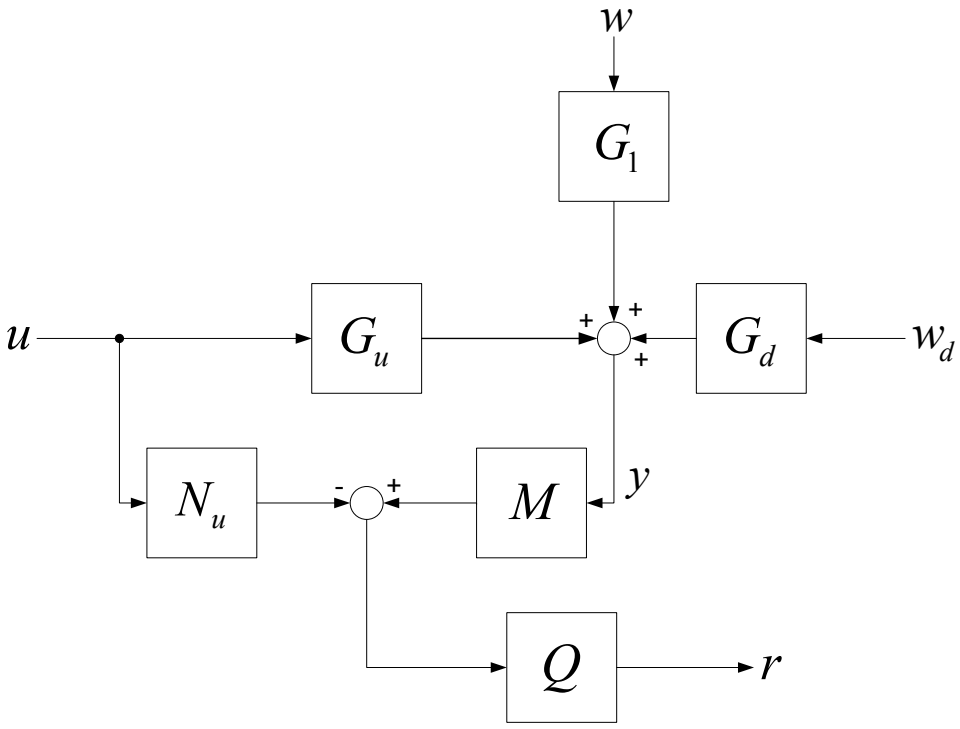

Figure 2.4 $\mathcal{H}_-/\mathcal{H}_\infty$ filtering problem.

Let $\gamma > 0$, be a given uncertainty rejection level. Find a stable transfer matrix $\boldsymbol{Q}(s) \in \mathcal{RH}_\infty$ in (2-21)-(2-23) such that $\|\boldsymbol{G_{rw}}(s)\|_\infty \leq \gamma$ and $\|\boldsymbol{G_{rd}}(s)\|_-$ is maximized, i.e.

$$\max_{\boldsymbol{Q}(s)\in\mathcal{RH}_\infty} \{\|\boldsymbol{Q}(s)\boldsymbol{N_d}(s)\|_- : \|\boldsymbol{Q}(s)\boldsymbol{N_1}(s)\|_\infty \leq \gamma\}.$$

By letting $\boldsymbol{R_1 = D_{21}D_{21}^T} > 0$ and letting $\boldsymbol{Y \geq 0}$ be the stabilizing solution to the following ARE:

$$\begin{aligned}&\boldsymbol{\left(A - B_1 D_{21}^T R_1^{-1} C\right)Y + Y(A - B_1 D_{21}^T R_1^{-1} C)^T - YC^T R_1^{-1} CY}\\&\boldsymbol{+B_1\left(I - D_{21}^T R_1^{-1} D_{21}\right)B_1^T = 0}\end{aligned} \tag{2-24}$$

such that $\boldsymbol{A - B_1 D_{21}^T R_1^{-1} C - YC^T R_1^{-1} C}$ is stable, we can define

$$\boldsymbol{L_0 = -\left(B_1 D_{21}^T + YC^T\right)R_1^{-1}}. \tag{2-25}$$

Then

$$\max_{\boldsymbol{Q}(s)\in\mathcal{RH}_\infty} \{\|\boldsymbol{Q}(s)\boldsymbol{N_d}(s)\|_- : \|\boldsymbol{Q}(s)\boldsymbol{N_1}(s)\|_\infty \leq \gamma\} = \gamma\left\|\boldsymbol{V^{-1}}(s)\boldsymbol{N_d}(s)\right\|_-$$

and an optimal filter can be found that has the following state space representation:

$$\boldsymbol{r = Q_{opt}}(s)[\boldsymbol{M}(s) \quad -\boldsymbol{N_u}(s)]\begin{bmatrix}\boldsymbol{y}\\ \boldsymbol{u}\end{bmatrix} \tag{2-26}$$

where

$$\boldsymbol{Q_{opt}}(s)[\boldsymbol{M}(s) \quad -\boldsymbol{N_u}(s)] = \gamma\left[\begin{array}{c|cc}\boldsymbol{A + L_0 C} & \boldsymbol{-L_0} & \boldsymbol{B + L_0 D}\\ \hline \boldsymbol{-R_1^{-1/2} C} & \boldsymbol{R_1^{-1/2}} & \boldsymbol{R_1^{-1/2} D}\end{array}\right]$$

and

$$\boldsymbol{V^{-1}}(s)\boldsymbol{N_d}(s) = \left[\begin{array}{c|c}\boldsymbol{A + L_0 C} & \boldsymbol{B_d + L_0 D_d}\\ \hline \boldsymbol{R_1^{-1/2} C} & \boldsymbol{R_1^{-1/2} D_d}\end{array}\right].$$

In other words, the optimal $\mathcal{H}_-/\mathcal{H}_\infty$ filter is the following observer:

$$\begin{aligned}&\boldsymbol{\dot{\hat{x}} = (A + L_0 C)\hat{x} - L_0 y + (B + L_0 D)u}\\&\boldsymbol{r = \gamma R_1^{-1/2}(y - C\hat{x} - Du)}.\end{aligned} \tag{2-27}$$

2.7 Permanent Magnet DC Motor Model

DC motors available both on the market and in use today can be found in a variety of types. These include separately excited DC motors, series DC motors, shunt DC motors, brushless DC motors (BLDC) and permanent magnet DC motors (PMDC) to name a few. In order to design a disturbance torque estimator, an appropriate nominal

mathematical model must first be developed. A PMDC, [25], is considered in this thesis. A schematic of a PMDC with no load is shown in *Figure 2.5*.

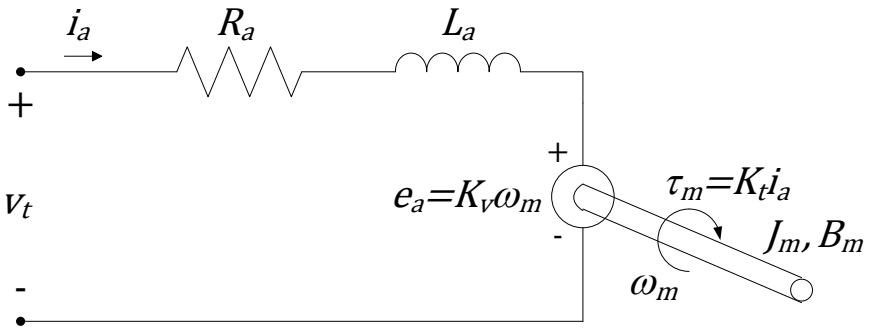

Figure 2.5 Schematic of a PMDC.

A nominal PMDC with no load can be represented by the following two coupled, linear, time-invariant, continuous-time, differential equations:

$$\begin{aligned} v_t &= R_a i_a + L_a \frac{di_a}{dt} + K_v \omega_m \\ K_t i_a &= J_m \frac{d\omega_m}{dt} + B_m \omega_m \end{aligned} \tag{2-28}$$

where the first equation is the electrical equation of the PMDC derived using Kirchhoff's voltage law and the second equation is the mechanical equation of the PMDC derived using Newton's second law of motion applied to a rotational system.

In general, by selecting the state variables to be i_a and ω_m and having the sole measurement output of the system be the armature current, a state space model for a PMDC can be written in the following form:

$$\begin{aligned} \dot{\boldsymbol{x}} &= \boldsymbol{A}\boldsymbol{x} + \boldsymbol{B}u \\ y &= \boldsymbol{C}\boldsymbol{x} \end{aligned} \tag{2-29}$$

where

$$\boldsymbol{A} = \begin{bmatrix} -\frac{R_a}{L_a} & -\frac{K_v}{L_a} \\ \frac{K_t}{J_m} & -\frac{B_m}{J_m} \end{bmatrix}, \qquad \boldsymbol{B} = \begin{bmatrix} \frac{1}{L_a} \\ 0 \end{bmatrix}, \qquad \boldsymbol{C} = [1 \quad 0], \qquad \boldsymbol{x} = \begin{bmatrix} i_a \\ \omega_m \end{bmatrix}, \qquad u = v_t, \qquad y = i_a.$$

By introducing disturbances and uncertainties into the system in the form of a disturbance torque and a disturbance voltage, [1], the equations in (2-28) can be rewritten as

$$\begin{aligned} v_t &= R_a i_a + L_a \frac{di_a}{dt} + K_v \omega_m + v_d \\ K_t i_a &= J_m \frac{d\omega_m}{dt} + B_m \omega_m + \tau_d \end{aligned} \tag{2-30}$$

where

$$\begin{aligned} v_d &= \Delta R_a i_a + \Delta L_a \frac{di_a}{dt} + \Delta K_v \omega_m \\ \tau_d &= -\Delta K_t i_a + \Delta J_m \frac{d\omega_m}{dt} + \Delta B_m \omega_m + \tau_L. \end{aligned} \tag{2-31}$$

A block diagram of a PMDC is shown in *Figure 2.*6.

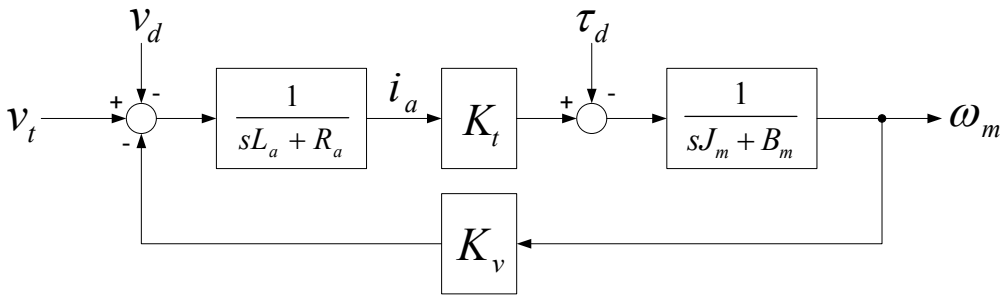

Figure 2.6 Block diagram of a PMDC.

It is worth noting that τ_L not only denotes the load torque, but also denotes any variations in the load that may arise as a result of other external disturbances acting on the motor's shaft. Also note that the state space model in (2-29) must be augmented in order to incorporate the appropriate disturbances and uncertainties, and that the state space models of the system that are required to design the estimator differ based on the filter type being employed. These augmentations will be discussed as part of the design of the disturbance torque estimators.

CHAPTER 3: DISTURBANCE TORQUE ESTIMATOR DESIGN[1]

3.1 Overall Disturbance Torque Estimator

The overall disturbance torque estimator consists of two parts: a state observer, and an equation that relates the disturbance torque estimation to the system states and their derivatives.

Assuming that the pair $(\boldsymbol{A}, \boldsymbol{C})$ is observable, an observer in the form of (2-2) can be designed. For the PMDC considered in this thesis, the observability matrix can be calculated as

$$\boldsymbol{\mathcal{O}} = \begin{bmatrix} \boldsymbol{C} \\ \boldsymbol{CA} \end{bmatrix} = \begin{bmatrix} 1 & 0 \\ -\frac{R_a}{L_a} & -\frac{K_v}{L_a} \end{bmatrix}. \tag{3-1}$$

It can be seen clearly in (3-1) that the observability matrix has full column rank and thus the PMDC considered here is an observable system.

By rearranging the mechanical equation of the PMDC in (2-30), the disturbance torque can be written as

$$\tau_d = K_t i_a - J_m \dot{\omega}_m - B_m \omega_m. \tag{3-2}$$

Since i_a is the only measurement output of the system and since the PMDC is an observable system, ω_m and $\dot{\omega}_m$ in (3-2) can be replaced with their respective estimates $\widehat{\omega}_m$ and $\dot{\widehat{\omega}}_m$. Thus an equation for the disturbance torque estimate can be written as

$$\hat{\tau}_d = K_t i_a - J_m \dot{\widehat{\omega}}_m - B_m \widehat{\omega}_m. \tag{3-3}$$

Note that the actual armature current is used as opposed to the estimated armature current since it is assumed that the measured value is more reliable than the estimated value.

[1] This chapter contains material that is the result of joint research.

The overall disturbance torque estimator is described by (2-2) and (3-3). A block diagram of the overall estimator is shown in *Figure 3.1* and a block diagram of a system with disturbance torque estimation is shown in *Figure 3.2*.

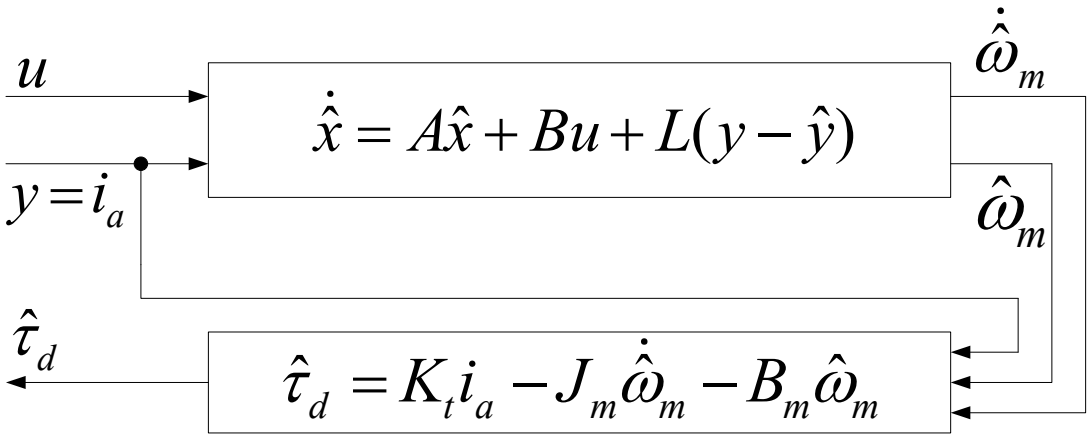

Figure 3.1 Disturbance torque estimator.

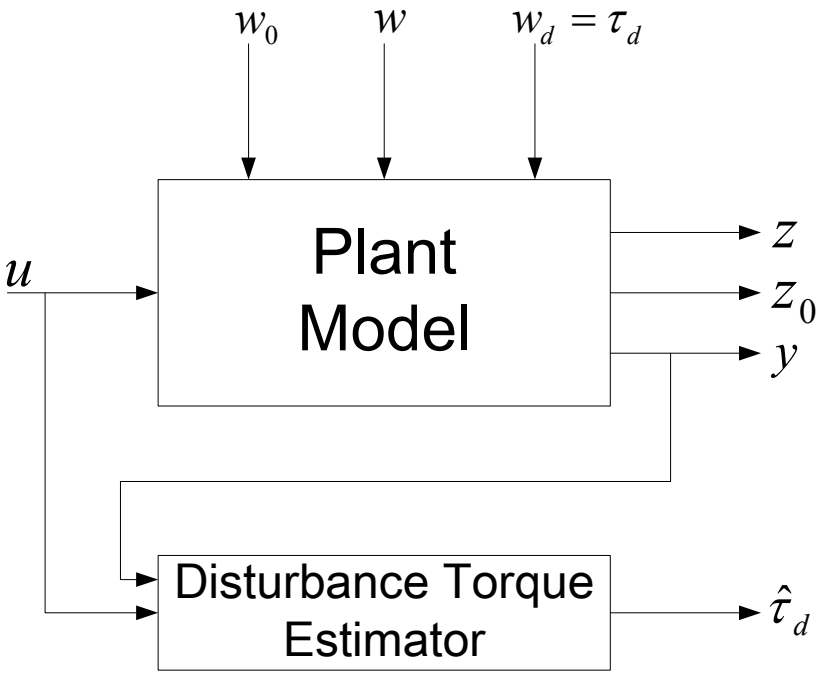

Figure 3.2 System with disturbance torque estimation.

3.2 $\mathcal{H}_\infty$ Filter System Model

In order to design an appropriate $\mathcal{H}_\infty$ filter to be used for disturbance torque estimation, the state space model of the PMDC in (2-29) must be augmented to include both the disturbance torque and model uncertainties. For the $\mathcal{H}_\infty$ filter, the state space model of the PMDC is written as:

$$\begin{aligned} \dot{\boldsymbol{x}} &= \boldsymbol{A}\boldsymbol{x} + \boldsymbol{B}u + \boldsymbol{B_d}w_d + \boldsymbol{B_1}\boldsymbol{w} \\ y &= \boldsymbol{C}\boldsymbol{x} \\ \boldsymbol{z} &= \boldsymbol{C_1}\boldsymbol{x} \end{aligned} \tag{3-4}$$

where $\boldsymbol{A}$, $\boldsymbol{B}$, $\boldsymbol{C}$, $\boldsymbol{x}$, u and y are the same as defined in (2-29) and

$$\boldsymbol{B_d} = \begin{bmatrix} 0 \\ -\dfrac{1}{J_m} \end{bmatrix}, \qquad \boldsymbol{C_1} = \begin{bmatrix} 1 & 0 \\ 0 & 1 \end{bmatrix}, \qquad w_d = \tau_d.$$

The structures of $\boldsymbol{B_1}$ and $\boldsymbol{w}$ change based on the combination of uncertainties being used to calculate the observer gain and will be discussed later in this chapter.

3.3 $\mathcal{H}_\infty$ Gaussian Filter System Model

In the case of the $\mathcal{H}_\infty$ Gaussian filter the state space model of the PMDC in (2-29) must be augmented to include not only the disturbance torque and model uncertainties, but to also include white noise. For the $\mathcal{H}_\infty$ Gaussian filter, the state space model of the PMDC is written as:

$$\begin{aligned} \dot{\boldsymbol{x}} &= \boldsymbol{A}\boldsymbol{x} + \boldsymbol{B}u + \boldsymbol{B_d}w_d + \boldsymbol{B_0}\boldsymbol{w_0} + \boldsymbol{B_1}\boldsymbol{w} \\ y &= \boldsymbol{C}\boldsymbol{x} + \boldsymbol{D_{20}}\boldsymbol{w_0} \\ \boldsymbol{z_0} &= \boldsymbol{C_0}\boldsymbol{x} \\ \boldsymbol{z} &= \boldsymbol{C_1}\boldsymbol{x} \end{aligned} \tag{3-5}$$

where $\boldsymbol{A}$, $\boldsymbol{B}$, $\boldsymbol{C}$, $\boldsymbol{x}$, u and y are the same as in (2-29) and

$$\boldsymbol{B_d} = \begin{bmatrix} 0 \\ -\dfrac{1}{J_m} \end{bmatrix}, \qquad \boldsymbol{C_0} = \begin{bmatrix} 1 & 0 \\ 0 & 1 \end{bmatrix}, \qquad \boldsymbol{C_1} = \begin{bmatrix} 1 & 0 \\ 0 & 1 \end{bmatrix}, \qquad w_d = \tau_d.$$

The structures of $\boldsymbol{B_0}$, $\boldsymbol{B_1}$, $\boldsymbol{w_0}$ and $\boldsymbol{w}$ also change based on the combination of uncertainties and white noises being used to calculate the observer gain and will be discussed later in this chapter and in chapter 5.

3.4 $\mathcal{H}_-/\mathcal{H}_\infty$ Filter System Model

Similar to the $\mathcal{H}_\infty$ filter, in the case of the $\mathcal{H}_-/\mathcal{H}_\infty$ filter the state space model of the PMDC in (2-29) must be augmented to include both the disturbance torque and model uncertainties. For the $\mathcal{H}_-/\mathcal{H}_\infty$ filter, the state space model of the PMDC is written as:

$$\begin{aligned} \dot{\boldsymbol{x}} &= \boldsymbol{A}\boldsymbol{x} + \boldsymbol{B}u + \boldsymbol{B_d}w_d + \boldsymbol{B_1}\boldsymbol{w} \\ y &= \boldsymbol{C}\boldsymbol{x} + \boldsymbol{D_{21}}\boldsymbol{w} \end{aligned} \tag{3-6}$$

where $\boldsymbol{A}$, $\boldsymbol{B}$, $\boldsymbol{C}$, $\boldsymbol{x}$, u and y are the same as defined in (2-29) and

$$\boldsymbol{B_d} = \begin{bmatrix} 0 \\ -\dfrac{1}{J_m} \end{bmatrix}, \qquad\qquad w_d = \tau_d.$$

The structures of $\boldsymbol{B_1}$, $\boldsymbol{D_{21}}$ and $\boldsymbol{w}$ change based on the combination of uncertainties being used to calculate the observer gain and will be discussed later in this chapter.

3.5 Performance Requirements and Error/Disturbance Relation

By defining $\boldsymbol{e_x} = \boldsymbol{x} - \hat{\boldsymbol{x}} = [e_i \quad e_\omega]^{\boldsymbol{T}}$ where e_i and e_ω denote the error in estimation of armature current and motor speed respectively, the error dynamics of the disturbance torque estimator can be defined when using an $\mathcal{H}_\infty$ filter as

$$\dot{\boldsymbol{e}}_{\boldsymbol{x}} = \dot{\boldsymbol{x}} - \dot{\hat{\boldsymbol{x}}} = (\boldsymbol{A} - \boldsymbol{LC})\boldsymbol{e_x} + \boldsymbol{B_d}w_d + \boldsymbol{B_1}\boldsymbol{w} \tag{3-7}$$

when using an $\mathcal{H}_\infty$ Gaussian filter as

$$\dot{\boldsymbol{e}}_{\boldsymbol{x}} = \dot{\boldsymbol{x}} - \dot{\hat{\boldsymbol{x}}} = (\boldsymbol{A} - \boldsymbol{LC})\boldsymbol{e_x} + \boldsymbol{B_d}w_d + (\boldsymbol{B_0} - \boldsymbol{LD_{20}})\boldsymbol{w_0} + \boldsymbol{B_1}\boldsymbol{w} \tag{3-8}$$

and when using an $\mathcal{H}_-/\mathcal{H}_\infty$ filter as

$$\dot{\boldsymbol{e}}_{\boldsymbol{x}} = \dot{\boldsymbol{x}} - \dot{\hat{\boldsymbol{x}}} = (\boldsymbol{A} - \boldsymbol{LC})\boldsymbol{e_x} + \boldsymbol{B_d}w_d + (\boldsymbol{B_1} + \boldsymbol{LD_{21}})\boldsymbol{w} \tag{3-9}$$

where $\boldsymbol{L} = [L_1 \quad L_2]^{\boldsymbol{T}}$ for the PMDC. Note that the gain $\boldsymbol{L_0}$ described previously for the $\mathcal{H}_-/\mathcal{H}_\infty$ filter, was defined solely for the purpose of derivation and can be considered the same as the gain $\boldsymbol{L}$ in (2-2) and is defined as

$$\boldsymbol{L} = \boldsymbol{L_0} = (\boldsymbol{B_1 D_{21}^T} + \boldsymbol{Y C^T})\boldsymbol{R_1^{-1}} \tag{3-10}$$

for the purpose of implementation.

Using (3-7), (3-8) and (3-9), certain criteria can be defined as to what the estimator should yield in terms of performance:

1. The design of the disturbance torque estimator must ensure that the eigenvalues of $(\boldsymbol{A} - \boldsymbol{LC})$ lie within the left-half plane. In other words, the estimator must be stable.
2. The disturbance torque estimator must provide an appropriate estimation of the disturbance torque.
3. The selection of the gain observer gain $\boldsymbol{L}$ must minimize or constrain the transfer function from uncertainty to error (and white noise to error in the case of the $\mathcal{H}_\infty$ Gaussian filter). In other words, the estimation must be robust to model uncertainties (and white noise in the case of the $\mathcal{H}_\infty$ Gaussian filter).

The first two criteria can be easily satisfied by a wide range of values for the observer gain. Using this knowledge, it can be assumed that there also exists within that range, an observer gain that also satisfies the third criterion. The difficulty arises in the determination of such a gain, which can be resolved using the calculation techniques discussed in this thesis.

Another issue that arises in the design of the disturbance torque estimator is that in the designs of both the $\mathcal{H}_\infty$ filter and the $\mathcal{H}_\infty$ Gaussian filter, there is no systematic treatment of the disturbance torque but rather only of the uncertainties and white noise.

This issue is addressed solely in the design of the $\mathcal{H}_-/\mathcal{H}_\infty$ filter thus justifying the use of such a filter design. The observer gain in this filter design not only constrains the transfer function from uncertainty to error but also amplifies the sensitivity of the transfer function from disturbance to error which in turn also amplifies the sensitivity of the estimation to the disturbance torque.

Since the value of the observer gain in all cases constrains the transfer function from uncertainty to error, and in the case of the $\mathcal{H}_\infty$ Gaussian filter also minimizes the impact of white noise, it can be assumed without loss of generality that (3-7), (3-8) and (3-9) can be reduced to

$$\dot{\boldsymbol{e}}_{\boldsymbol{x}} = (\boldsymbol{A} - \boldsymbol{LC})\boldsymbol{e}_{\boldsymbol{x}} + \boldsymbol{B}_{\boldsymbol{d}} w_d. \tag{3-11}$$

Solving (3-11) yields

$$\boldsymbol{e}_{\boldsymbol{x}} = e^{(\boldsymbol{A}-\boldsymbol{LC})t}\boldsymbol{e}_{\boldsymbol{x}}(\boldsymbol{0}) + \int_0^t e^{(\boldsymbol{A}-\boldsymbol{LC})(t-\tau)}\boldsymbol{B}_{\boldsymbol{d}} w_d(\tau)d\tau. \tag{3-12}$$

It can be seen in (3-12) that under steady-state conditions, the estimation error is related to the disturbance. Note that steady-state can refer to a periodic steady-state such as sinusoidal steady state. Since this equation does not assume a constant disturbance, it can be said that with an observer gain calculated using the methods described in this thesis, it is possible to estimate a non-constant disturbance that varies with time at low frequency, i.e., the period of the disturbance should not exceed the time it takes for the error dynamics to settle. In other words, for a non-constant disturbance, the dynamics of the disturbance should not be faster than the dynamics of the estimation error.

For a PMDC, if the observer state estimation equation for $\dot{\hat{\omega}}_m$ is substituted into (3-3), the disturbance torque estimation equation becomes:

$$\hat{\tau}_d = (K_t - L_2 J_m)e_i \tag{3-13}$$

where $e_i = i_a - \hat{\imath}_a$. Thus we can see from (3-12) and (3-13) that that disturbance torque is related to the error in estimation of the armature current and can be estimated without the assumption of the disturbance torque being constant. This justifies the need to constrain the transfer function from uncertainty to disturbance, minimize the impact of white noise on the error and amplify the transfer function from disturbance to error.

3.6 Residual/Disturbance Relation

In order to fully implement a disturbance torque estimator that is built using an $\mathcal{H}_-/\mathcal{H}_\infty$ filter, a relation between the error in estimation of armature current and the residual signal must be found since the $\mathcal{H}_-/\mathcal{H}_\infty$ filter described in this thesis operates on the transfer functions from disturbance to residual and uncertainty to residual. Using the residual equation from (2-27) and the output equation from (3-6) we find that

$$r = \gamma \boldsymbol{R_1^{-1/2} C e_x} + \gamma \boldsymbol{R_1^{-1/2} D_{21} w}. \tag{3-14}$$

Since the filter is designed to constrain the transfer function from uncertainty to residual, it can also be assumed without loss of generality that (3-14) can be reduced to

$$r = \gamma \boldsymbol{R_1^{-1/2} C e_x}. \tag{3-15}$$

Substituting the value of $\boldsymbol{C}$ into (3-15) and rearranging results in

$$e_i = \frac{r}{\gamma R_1^{-1/2}}. \tag{3-16}$$

Substituting (3-16) into (3-13) results in

$$\hat{t}_d = (K_t - L_2 J_m)\frac{r}{\gamma R_1^{-1/2}}. \tag{3-17}$$

It can be easily seen that (3-3) and (3-17) are equivalent and thus the complete disturbance torque estimator designed using an $\mathcal{H}_-/\mathcal{H}_\infty$ filter can be entirely described by (2-2) (with $\boldsymbol{D} = \boldsymbol{0}$) and (3-3) as is also the case for the estimators designed using an $\mathcal{H}_\infty$ filter and an $\mathcal{H}_\infty$ Gaussian filter.

3.7 Cases for Design

In order to properly calculate an observer gain that produces a robust estimation, the parameters of interest for which the estimation must be robust against must first be defined. Since the disturbance torque being estimated is assumed to either be constant or to vary with low frequency, the armature current may also be assumed to either be constant or to vary with low frequency. As a result, the term $\Delta L_a\,(di_a/dt)$ can be assumed to be small and negligible, i.e., any variations in the armature inductance can be ignored. Also, as shown in (2-31), variations in any of the mechanical parameters of the motor and variations in the load can be considered as part of the disturbance torque. As a result, the only two model uncertainties of significance are variations in the armature resistance and variations in the electrical constant. From this, three separate cases for the structures of $\boldsymbol{B_1}$, $\boldsymbol{D_{21}}$ and $\boldsymbol{w}$ can be considered.

In case 1, only variations in the armature resistance are considered. In case 2, only variations in the electrical constant are considered. In case 3, both variations in the armature resistance and the electrical constant are considered. The cases are summarized in *Table 3.1*. Note that in all cases w_1, w_2 and w_3 are positive constants that represent the significance of the particular uncertainty. They are added to the system in order to influence the calculation of the observer gain.

In the case of the $\mathcal{H}_-/\mathcal{H}_\infty$ filter, another model uncertainty was also required to ensure that there exists a solution to the ARE in (2-24). Since $\boldsymbol{R_1} = \boldsymbol{D_{21}}\boldsymbol{D_{21}^T} > 0$, it is required to define some sort of output uncertainty so that the matrix $\boldsymbol{D_{21}}$ can be defined and thus result in $\boldsymbol{R_1} > 0$. For this purpose, the parameter Δi_a is defined to represent measurement output uncertainty. This is justified by the fact that in real physical systems, no measurement is ever completely accurate and always contains some

amount of uncertainty. Thus we redefine the measurement output for the $\mathcal{H}_-/\mathcal{H}_\infty$ filter as $y = i_a + \Delta i_a$ and assume that the armature current being measured contains within it some amount of uncertainty.

Once determined, these parameters are used to solve the ARE's in (2-6), (2-13), (2-14) and (2-24) whose solutions are then used to calculate the corresponding observer gains (2-7), (2-15) and (3-10).

Table 3.1 Structures of $\boldsymbol{B_1}$, $\boldsymbol{D_{21}}$ and $\boldsymbol{w}$.

Case	**$\mathcal{H}_\infty$ and $\mathcal{H}_\infty$ Gaussian Filters**	**$\mathcal{H}_-/\mathcal{H}_\infty$ Filter**
1	$w = \Delta R_a i_a$, $\boldsymbol{B_1} = \begin{bmatrix} -\frac{w_1}{L_a} \\ 0 \end{bmatrix}$	$\boldsymbol{w} = \begin{bmatrix} \Delta R_a i_a \\ \Delta i_a \end{bmatrix}$, $\boldsymbol{B_1} = \begin{bmatrix} -\frac{w_1}{L_a} & 0 \\ 0 & 0 \end{bmatrix}$, $\boldsymbol{D_{21}} = [0 \quad w_3]$
2	$w = \Delta K_v \omega_m$, $\boldsymbol{B_1} = \begin{bmatrix} -\frac{w_2}{L_a} \\ 0 \end{bmatrix}$	$\boldsymbol{w} = \begin{bmatrix} \Delta K_v \omega_m \\ \Delta i_a \end{bmatrix}$, $\boldsymbol{B_1} = \begin{bmatrix} -\frac{w_2}{L_a} & 0 \\ 0 & 0 \end{bmatrix}$, $\boldsymbol{D_{21}} = [0 \quad w_3]$
3	$\boldsymbol{w} = \begin{bmatrix} \Delta R_a i_a \\ \Delta K_v \omega_m \end{bmatrix}$, $\boldsymbol{B_1} = \begin{bmatrix} -\frac{w_1}{L_a} & -\frac{w_2}{L_a} \\ 0 & 0 \end{bmatrix}$	$\boldsymbol{w} = \begin{bmatrix} \Delta R_a i_a \\ \Delta K_v \omega_m \\ \Delta i_a \end{bmatrix}$, $\boldsymbol{B_1} = \begin{bmatrix} -\frac{w_1}{L_a} & -\frac{w_2}{L_a} & 0 \\ 0 & 0 & 0 \end{bmatrix}$, $\boldsymbol{D_{21}} = [0 \quad 0 \quad w_3]$

CHAPTER 4: HARDWARE AND SOFTWARE CONFIGURATION

In order to test the designed disturbance torque estimators, a real-time hardware test bench was setup. The test bench consisted of the following components:

1. A PMDC used as the motor under test (MUT).
2. A PMDC used as a dyno in order to provide disturbance torques to the MUT.
3. A current shunt resistor along with signal conditioning circuitry used to measure the armature current of the MUT.
4. An in-line torque sensor used to validate the disturbance torque estimations.
5. Two H-bridge controllers used to control the input voltage of the MUT and the dyno motor.
6. A real-time (RT) computer used to implement the disturbance torque estimators, generate inputs for the H-bridge controllers and acquire data from the sensors.
7. An operating station used to develop models of the disturbance torque estimators for execution on the RT computer, interface with the RT-computer, control the execution of tests, and plot and analyze experimental data.

A block diagram of the test bench is shown in *Figure 4.1*.

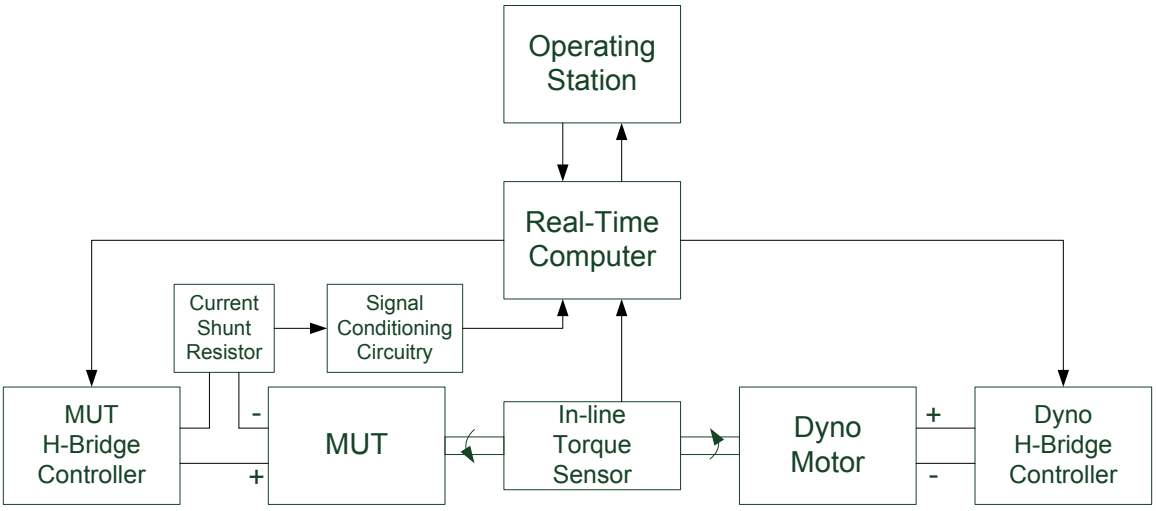

Figure 4.1 Block diagram of the real-time hardware test bench.

4.1 Determination of Parameters of DC Motor Under Test

Prior to testing the estimators, the parameters of the plant, in this case the PMDC, must be determined so that calculation of observer gains may be conducted, and also so that the estimator models can be programmed into the RT computer. For the PMDC, these parameters include the motor's armature resistance, armature inductance, electrical constant, mechanical constant, viscous friction coefficient and inertial coefficient. These parameters can either be found in a datasheet that is provided by the manufacturer, or can be determined through testing.

If testing is to be performed in order to determine these parameters, the model of the model of the PMDC that is used is in the form of (2-28) where no disturbance, uncertainty, or noise is considered in the system. Each test is repeated 2-3 times and the results are averaged.

All of the values that are obtained either from documentation or from testing are assumed to be nominal values. Any uncertainty or variations in the parameters are addressed in the design of the estimators.

4.1.1 Armature Resistance

The first step in determining the armature resistance of a PMDC is to lock the armature so that $\omega_m = 0$ regardless of the input to the motor. A small, known voltage, v_t, is then applied to the motor and the armature current is measured after reaching steady-state ($di_a/dt = 0$). This must be done quickly in order to prevent the armature winding from heating up which could cause a change in its resistance. Using the known value of v_t and the measured value of i_a, the armature resistance can be calculated as

$$R_a = \frac{v_t}{i_a}. \tag{4-1}$$

4.1.2 Armature Inductance

To determine the armature inductance of a PMDC, the armature is to be locked once again so that $\omega_m = 0$ regardless of the input to the motor. A resistor of known resistance, R_k, is then connected in series with armature circuit. A step voltage is applied to the motor and the transient response of the voltage across R_k is plotted. This must also be done quickly in order to prevent the armature winding from heating up. The electrical time constant, τ_E, is then determined from the transient response. Using the value of R_a that has already been obtained, the known value of R_k and the measured value of τ_E, the armature inductance can be calculated as

$$L_a = \tau_E(R_a + R_k). \tag{4-2}$$

4.1.3 Electrical Constant and Mechanical Constant

In determining the electrical constant, the PMDC is allowed to run freely with no load attached to it. A small known voltage, v_t, is applied to the motor and the armature current and motor speed are measured after reaching steady-state ($di_a/dt = 0$ and $d\omega_m/dt = 0$). Once again this must be done quickly in order to prevent the armature winding from heating up. Using the known value of v_t, the previously determined value of R_a and the measured values of i_a and ω_m, the electrical constant can be calculated as

$$K_v = \frac{v_t - R_a i_a}{\omega_m}. \tag{4-3}$$

The value of the mechanical constant can be easily determined if using SI units to measure and calculate the electrical constant. This results from the fact that in SI units, the value of the mechanical constant is equivalent to the value of the electrical constant. Thus the value of the mechanical constant can be calculated as

$$K_t = K_v. \tag{4-4}$$

4.1.4 Viscous Friction Coefficient

To determine the viscous friction coefficient, the PMDC is once again allowed to run freely with no load attached to it. A small known voltage, v_t, is applied to the motor and the armature current and motor speed are measured after reaching steady-state ($di_a/dt = 0$ and $d\omega_m/dt = 0$). Using the previously determined value of K_t and the measured values of i_a and ω_m, the viscous friction coefficient can be calculated as

$$B_m = \frac{K_t i_a}{\omega_m}. \tag{4-5}$$

4.1.5 Inertial Coefficient

In determining the inertial coefficient, the PMDC is once again allowed to run freely with no load attached to it. A step voltage, v_t, whose magnitude is the rated input voltage of the PMDC is applied to the motor so that it runs at rated speed and the transient response of the motor speed is plotted. The mechanical time constant, τ_M, is then determined from the transient response. Using the previously determined value of B_m and the measured value of τ_M, the inertial coefficient can be calculated as

$$J_m = \tau_M B_M. \tag{4-6}$$

4.2 Hardware Configuration

Each component of the test bench is designed to perform specific tasks and as such has its own separate requirements and specifications that must be satisfied in order to make proper use of the particular component. These specifications can include such things as power ratings, shielding requirements, operating temperatures and wiring configurations. Other components may require programming, mode selection or calibration in order to function in the desired manner and to produce the correct output.

When performing data acquisition, it is necessary to relate the output of the sensor to the measured quantity. In many situations, this relation is provided by the manufacturer. Other times the sensor must be tested and calibrated in order to determine this relation. Signal conditioning of the sensor output may also be required in some situations in order to ensure that the sensor output is compatible with the data acquisition hardware. All of these tasks must be performed prior to the conducting of any tests to ensure that testing and experimentation can be performed effectively.

4.2.1 Operating Station and Real-Time Computer

The hardware test bench has two computers used to develop models, manage the execution of tests, analyze data and implement algorithms. Model development, test management and data analysis are taken care of by an operating station consisting of a Dell Dimension 4550 computer shown in *Figure 4.2*. Implementation of algorithms is handled by an Opal-RT real-time computer shown in *Figure 4.3*. The specifications of the operating station and the RT computer are listed in *Table 4.1*.

Figure 4.2 Operating station.

Figure 4.3 RT computer.

Table 4.1 Operating station and RT computer specifications.

Device	**Operating Station**	**RT Computer**
Operating System	Windows XP Service Pack 2	QNX 6.0
Processor	Intel Pentium 4 CPU at 1.80 GHz	2 Intel 686 2401 MHz FPU's
Memory	512 MB DDR SDRAM	1015 MB RAM
Hard Drive	60 GB HDD	HDD
Network Interface Card	Realtek RTL8139 Family PCI Fast Ethernet NIC	Netlink BCM5787M Gigabit Ethernet PCI Express

The operating station and the RT computer are networked together using a Local Area Network (LAN) consisting of a standard Ethernet cable that connects directly between the network cards on both computers. The network uses the popular TCP/IP protocol to pass information back and forth between the two computers with the RT computer having an IP address of 192.168.10.101. This connection is detected automatically by the operating system on the operating station when both computers are on.

Interfacing between the RT computer and test components is handled by two terminal block interface modules shown in *Figure 4.4*. One module handles signals sent

from the RT computer to the test components while the second handles signals received from the test components. Each terminal block connects to an interface card via a 40-pin ribbon cable. One interface card is used to output analog voltages in the range of 0 V to +5 V while the second card is used to read in analog voltages in the range of -10 V to +10 V.

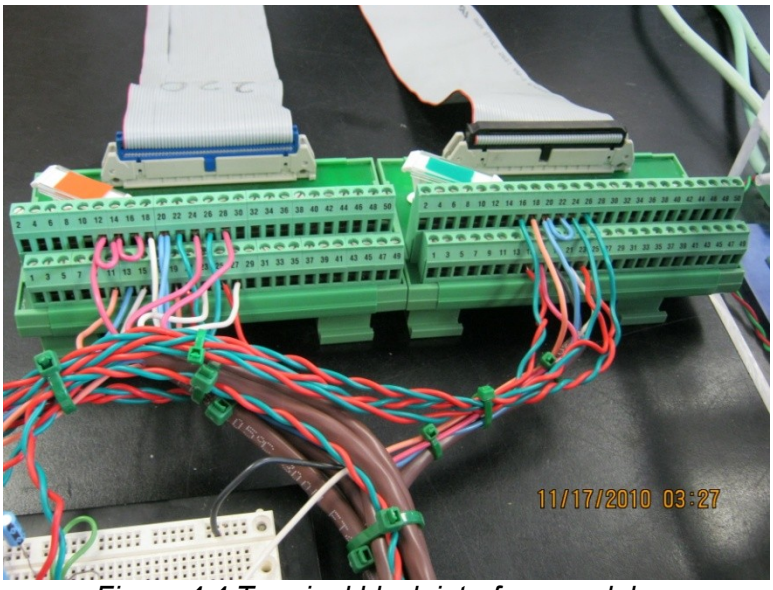

Figure 4.4 Terminal block interface modules.

4.2.2 Motor Under Test

The motor that is to be used to test the disturbance torque estimators is the Baldor CDP3440-V24 PMDC. The motor's ratings are listed in *Table 4.2* (see [26]) and the motor is shown in *Figure 4.5*. The parameters of this motor that are used in the estimator designs are given in chapter 5.

Table 4.2 Rated values of the motor under test.

Specification	**Rated Value**
Armature Voltage	24 V
Armature Current	29.4 A
Power	0.75 hp
Speed	1800 RPM
Full-Load Torque	3 N·m

Figure 4.5 PMDC used to test the disturbance torque estimators.

4.2.3 Dyno Motor

The motor that is to be used as a dyno to provide disturbance torques to the MUT is the Bosch GPA 12 V 400 W PMDC. The motor's ratings are listed in *Table 4.3* (see [27]) and the motor is shown in *Figure 4.6*.

Table 4.3 Rated values of the dyno motor.

Specification	**Rated Value**
Armature Voltage	12 V
Armature Current	50 A
Power	400 W
Speed	3400 RPM
Continuous Torque	1.2 N·m

Figure 4.6 Dyno motor used to generate disturbance torques.

4.2.4 Motor Controllers

The RoboteQ AX1500-BP, [28], and RoboteQ AX3500-BP, [29], motor controllers are used to control the input voltage to the MUT and dyno motor respectively. Each module can be powered by a 12-to-40 VDC power supply and is capable of acting as a stand-alone closed-loop controller, or as an H-bridge. The output of the controllers in all operating modes is in the form of a PWM signal. The AX1500-BP is shown in *Figure 4.7* and the AX3500-BP is shown in *Figure 4.8*.

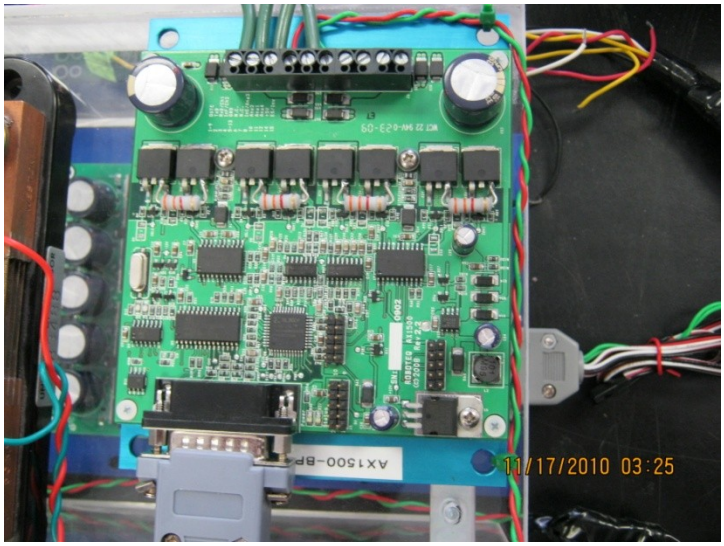

Figure 4.7 Motor under test controller.

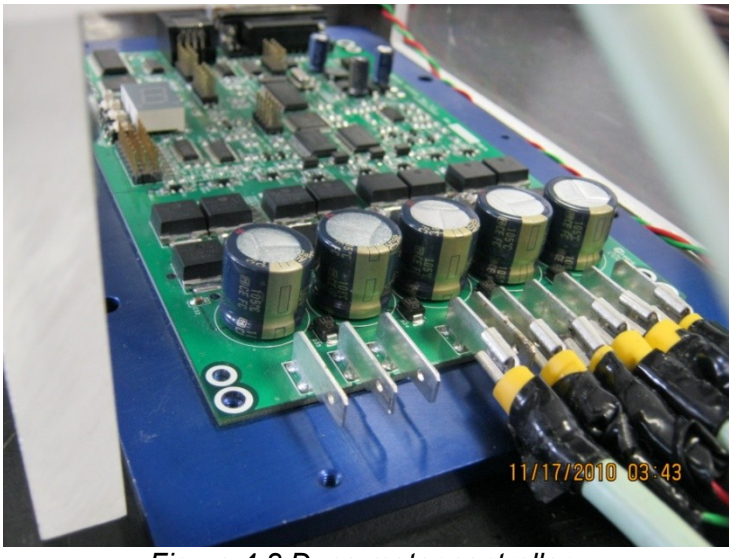

Figure 4.8 Dyno motor controller.

For the purposes of testing the disturbance torque estimators, the controllers are configured to operate using the analog signal input command mode and the open-loop, separate speed control mode. Using these settings allows the controller to operate the motors in either the forward or reverse direction in proportion to an analog input voltage that is to be provided from the RT computer. The analog input voltage must be in the range of 0 V to +5 V. These analog input voltages are translated into digital values that the controller then uses to set both the direction the motor will spin and the duty cycle of the PWM signal. A +2.5 V input translates into a digital value of 0 (motor off) while a +5 V input translates into a digital value of +127 (maximum forward command) and a 0 V input translates into a digital value of -127 (maximum reverse command).

In order to calculate the voltage being applied to the terminals of the test motor for use in the disturbance torque estimators, the following equation is used:

$$v_t = -9.6v_c + 24. \tag{4-7}$$

Note that (4-7) is not a fixed relation and changes depending upon the supply voltage used to power the controller.

4.2.5 Current Measurement

Since the disturbance torque estimators require a measurement of the armature current of the MUT, a current shunt resistor is used as a sensor to acquire this value. It is connected in series with the armature circuit of the MUT and has a nominal resistance that is small enough to be considered not to have a significant, or even any effect on the motor's performance. The current shunt that is to be used for testing has a rated output voltage of 50 mV at a rated current of 100 A which translates into a nominal resistance of 0.5 mΩ. It is shown in *Figure 4.9*.

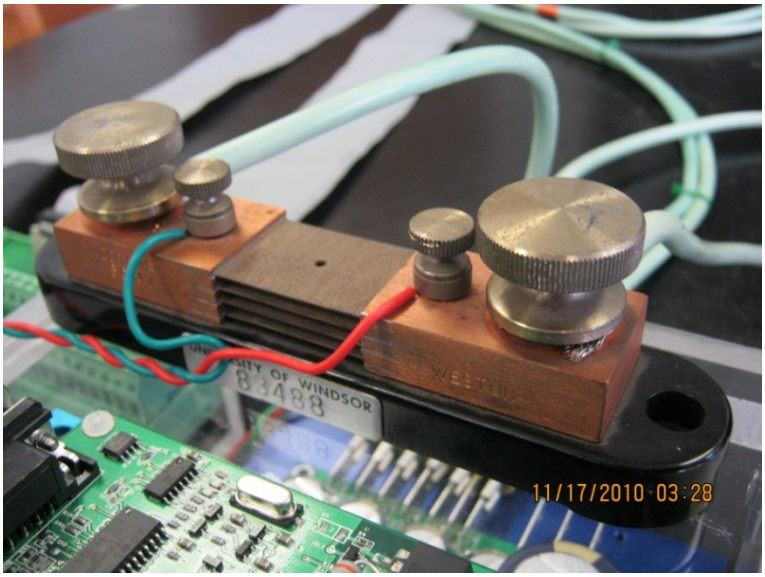

Figure 4.9 Current shunt resistor.

By measuring the voltage across the current shunt resistor, the armature current can be calculated. Before this can be done, the output voltage must be passed through signal conditioning circuitry in order to amplify it to a level that can be easily read-in by the RT computer. For this purpose, an instrumentation amplifier is used due to its superior noise rejection properties in comparison to the conventional op-amp. The output of the amplifier is also fed through a 1 kHz low-pass RC filter. The cut-off frequency of the filter was chosen to correspond with the 1 ms sampling period of the RT computer. The armature current can then be calculated as

$$i_a = \frac{v_o}{GR_s}. \tag{4-8}$$

4.2.6 Torque Sensor

In order to validate the disturbance torque estimations generated using the designed estimators, an in-line torque sensor, [30], is used. The sensor is connected in between the MUT and dyno motor to form one continuous shaft. It contains a strain gauge sensor as well as the appropriate signal conditioning circuitry. The sensor

measures the torque applied to its shaft and produces a mV/V output for a given torque. The torque sensor is shown in *Figure 4.10*.

Figure 4.10 In-line torque sensor.

The measured torque is related to the measured output voltage of the torque sensor as follows:

$$\tau_s = (0.7243 + 0.00007v_s)v_s. \quad (4\text{-}9)$$

4.2.7 Rotary Incremental Encoder

Determination of some of the parameters of the MUT requires a measurement of the motor's speed. These measurements are acquired with the use of a rotary incremental encoder (see [31]). The encoder has three output channels whose outputs can be used for either RSE measurements or differential measurements and allows for calculation of not only speed, but also of position and direction. The encoder is shown in *Figure 4.11*.

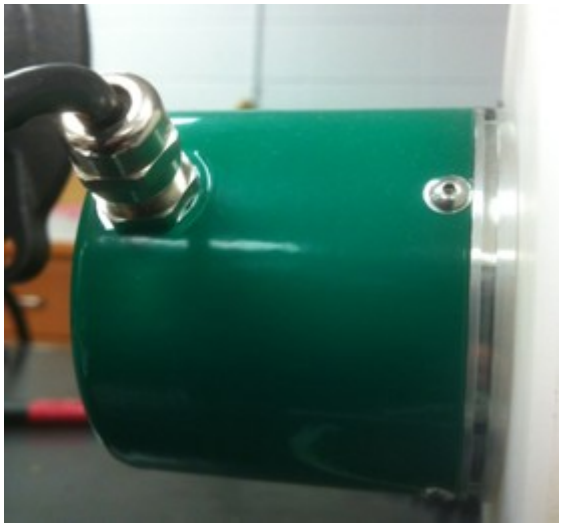

Figure 4.11 Rotary incremental encoder.

For the purpose of measuring motor speed, only one of the output channels is used. This channel is known as the index or Z channel. It outputs a pulse with a magnitude of +5 V once per revolution. By counting the number of pulses in a specified time interval, the speed of the motor can be calculated in radians per second as

$$\omega_m = \frac{2\pi \frac{N_E}{P_R}}{T_i} \tag{4-10}$$

where $P_R = 1$ for the index channel.

4.3 Software Configuration

Prior to testing the designed disturbance torque estimators, the various observer gains need to be determined and the models of the estimators must be input, compiled and programmed into both the operating station and the RT computer. Several software packages exist that can assist with these tasks. These packages aid in reducing the difficulty of the calculations involved in the designs, reduce the amount of time it takes to develop the software necessary for testing, and simplify both the acquisition and analysis of experimental data.

4.3.1 MATLAB/Simulink

Calculation of the various observer gains is performed in the MATLAB environment. This popular software can be used for many purposes ranging from simple calculations to complex analysis and visualization of data. In this environment, model parameters are input into a main program that calls on several different functions. Each function is designed to calculate a particular observer gain and when called upon, returns the value of the resulting observer gain matrix. The resulting eigenvalues of the error dynamics of each estimator are also calculated to ensure that stability requirements are satisfied.

The disturbance torque estimator models that are to be tested are created using a component of MATLAB known as Simulink. This environment allows for the creation, simulation and implementation of model-based designs. The models are input as block diagram representations of the mathematical equations associated with the system. Simulink contains many built-in ODE solvers that can be tuned to optimize the performance of the simulation. Since the estimators are to be implemented on an RT computer and the tests will be conducted in real-time, the simulation parameters are selected such that a fixed-step ODE solver is used. The solver is configured to have a fixed step size of 1 ms which corresponds to the sampling period of the RT computer.

4.3.2 RT-Lab

Once the disturbance torque estimator models are created and are ready for testing, the appropriate C-language code must be generated from the models and compiled in order to be programmed into the RT computer. A software package known as RT-Lab, [32], handles these tasks. This software communicates with MATLAB and

Simulink to open the models, generate and compile the necessary code, transfer the code to the RT computer, execute the tests and collect test data upon completion.

During execution, various test signals can be visualized and inputs to the system can be adjusted. This allows the user to execute and manipulate the magnitude and type of disturbance torque signals to be used for testing in real-time and without having to halt the current test being performed. Once a test is complete, the software communicates over the LAN to acquire all of the test data that was collected and stored by the RT computer. This data can then be plotted and analyzed in the MATLAB environment.

CHAPTER 5: TEST RESULTS[2]

5.1 Motor Under Test Parameters

The MUT's parameters, with the exception of armature resistance and armature inductance, were determined through testing of the motor according to the test procedures described in Chapter 4 and are listed in *Table 5.1*. The armature resistance and armature inductance were obtained from [26]. These parameters were then used to calculate the observer gains and in the estimation algorithms.

Table 5.1 Parameters of the motor under test.

Parameter	**Value**
Armature Resistance	0.0933 Ω
Armature Inductance	0.7493 mH
Electrical Constant	0.11235 V/rad/s
Mechanical Constant	0.11235 N·m/A
Viscous Friction Coefficient	1.2404×10^{-3} N·m/rad/s
Inertial Coefficient	1.8078×10^{-4} kg/m^2

5.2 Parameters Used for Observer Gain Calculation and Calculated Gains

In order to calculate the observer gains, all of the design parameters, i.e., γ, w_1, w_2 and w_3 as shown in *Table 3.1*, for each filter needed to be determined. These parameters were selected in such a way as to maintain a high level of robustness in the estimations, while also ensuring that stable solutions to the ARE's in (2-6), (2-13), (2-14) and (2-24) exist. The parameters are listed in *Table 5.2* and the resulting observer gains are listed in *Table 5.3*. Note that in all cases for the $\mathcal{H}_\infty$ Gaussian filter, $\boldsymbol{B_0}$, $\boldsymbol{D_{20}}$ and $\boldsymbol{w_0}$ were as follows:

$$\boldsymbol{B_0} = \begin{bmatrix} -\frac{0.5}{L_a} & 0 \\ 0 & 0 \end{bmatrix}, \quad \boldsymbol{D_{20}} = [0 \quad 1], \quad \boldsymbol{w_o} = \begin{bmatrix} V_{brush} \\ i_{a_{noise}} \end{bmatrix}.$$

[2] This chapter contains material that is the result of joint research.

Table 5.2 Parameters used to determine the observer gains.

Case	Parameter	$\mathcal{H}_\infty$ Filter	$\mathcal{H}_\infty$ Gaussian Filter	$\mathcal{H}_-/\mathcal{H}_\infty$ Filter
1	γ	10	50	10
	w_1	1	1	1
	w_2			
	w_3			1
2	γ	10	50	10
	w_1			
	w_2	0.5	0.5	0.5
	w_3			1
3	γ	10	50	10
	w_1	0.5	0.5	0.5
	w_2	0.5	0.5	0.5
	w_3			1

Table 5.3 Observer gains.

Case	$\mathcal{H}_\infty$ Filter	$\mathcal{H}_\infty$ Gaussian Filter	$\mathcal{H}_-/\mathcal{H}_\infty$ Filter
1	$\boldsymbol{L} = \begin{bmatrix} 1.26 \times 10^3 \\ -0.37 \times 10^3 \end{bmatrix}$	$\boldsymbol{L} = \begin{bmatrix} 5.51 \times 10^2 \\ 0.25 \times 10^2 \end{bmatrix}$	$\boldsymbol{L} = \begin{bmatrix} 1.21 \times 10^3 \\ 0.05 \times 10^3 \end{bmatrix}$
2	$\boldsymbol{L} = \begin{bmatrix} 5.61 \times 10^2 \\ -0.20 \times 10^2 \end{bmatrix}$	$\boldsymbol{L} = \begin{bmatrix} 5.49 \times 10^2 \\ 0.24 \times 10^2 \end{bmatrix}$	$\boldsymbol{L} = \begin{bmatrix} 5.49 \times 10^2 \\ 0.24 \times 10^2 \end{bmatrix}$
3	$\boldsymbol{L} = \begin{bmatrix} 8.43 \times 10^2 \\ -0.79 \times 10^2 \end{bmatrix}$	$\boldsymbol{L} = \begin{bmatrix} 5.50 \times 10^2 \\ 0.25 \times 10^2 \end{bmatrix}$	$\boldsymbol{L} = \begin{bmatrix} 8.22 \times 10^2 \\ 0.36 \times 10^2 \end{bmatrix}$

5.3 Input Patterns

For each of the cases, two distinct voltage input patterns were used to generate the disturbance torque. The first pattern consisted of a combination of constant and low frequency signals. This pattern was used to test not only that the estimators deliver appropriate results, but also to test for robustness and noise rejection. The second pattern consisted of a staircase that increased in small increments. This pattern was used to test for sensitivity. The patterns are shown in *Figure 5.1* and *Figure 5.2*. Note that these patterns represent the signal applied to the input of the dyno motor's controller. The actual input voltage applied to the dyno motor can be calculated using as

$$v_{dyno} = -4.8 v_{cdyno} + 12. \tag{5-1}$$

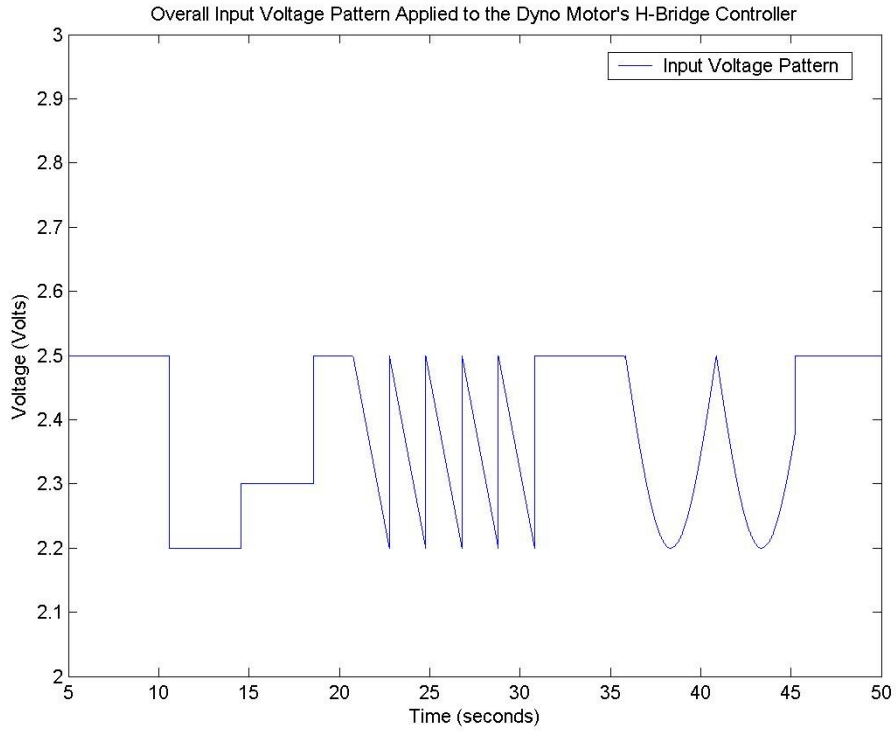

Figure 5.1 Overall input pattern.

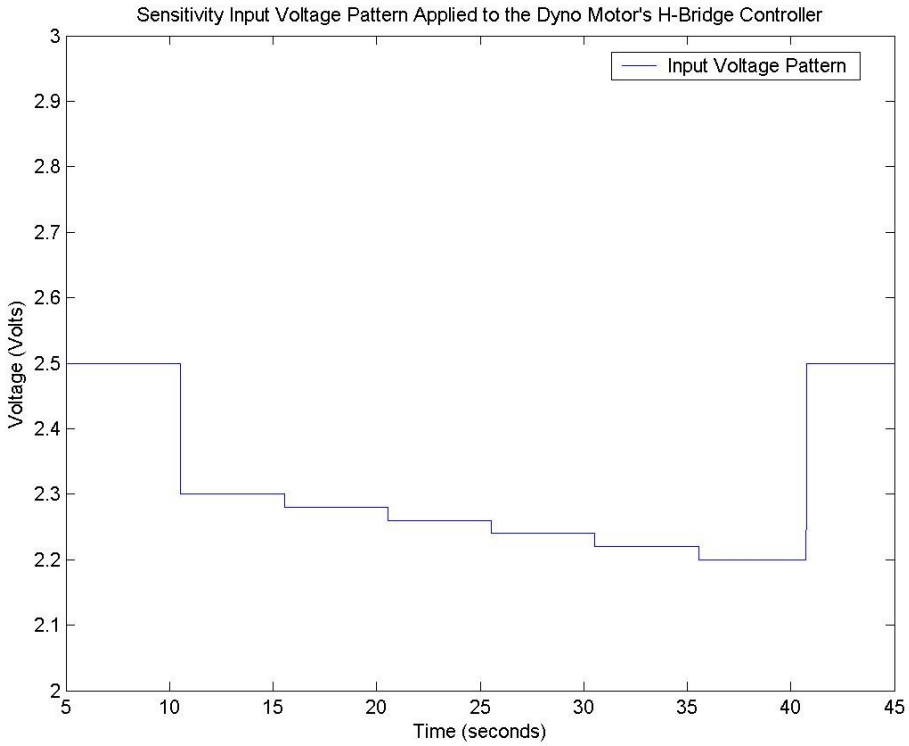

Figure 5.2 Sensitivity input pattern.

5.4 Disturbance Torque Estimation Test Results

For all of the tests, the estimators were implemented using both nominal parameters as well as parameters with the appropriate variations, as shown in *Table 3.1*, and the results were compared. All of the estimations were validated using the in-line torque sensor appropriately. Each test was conducted in real-time with the disturbance torque estimators implemented using the RT computer. Upon completion of a test, the data acquired by the RT computer was transmitted to the operating station. This data was then plotted using the MATLAB environment and analyzed to ensure that the estimators performed according to the design specifications.

5.4.1 Test Results for Case 1

For case 1, the tests were executed using nominal parameters and in the presence of variations in the armature resistance of ±10%. The first input pattern was used to generate the disturbance torque. The results for the $\mathcal{H}_\infty$, $\mathcal{H}_\infty$ Gaussian and $\mathcal{H}_-/\mathcal{H}_\infty$ disturbance torque estimations are shown in *Figure 5.3*, *Figure 5.4* and *Figure 5.5* respectively. These results were also magnified to show the robustness and noise rejection capabilities of the designed estimators and are shown in *Figure 5.6* and *Figure 5.7* respectively. Note that the noise rejection results are shown only for the estimation with nominal parameters for the purpose of clarity. Similar results appear in the presence of uncertainties.

The second input pattern was used to test the sensitivity requirement of the $\mathcal{H}_-/\mathcal{H}_\infty$ disturbance torque estimator. The results are shown in *Figure 5.*8. Once again note that the sensitivity results are shown only for the estimation with nominal parameters for the purpose of clarity. Similar results appear in the presence of uncertainties.

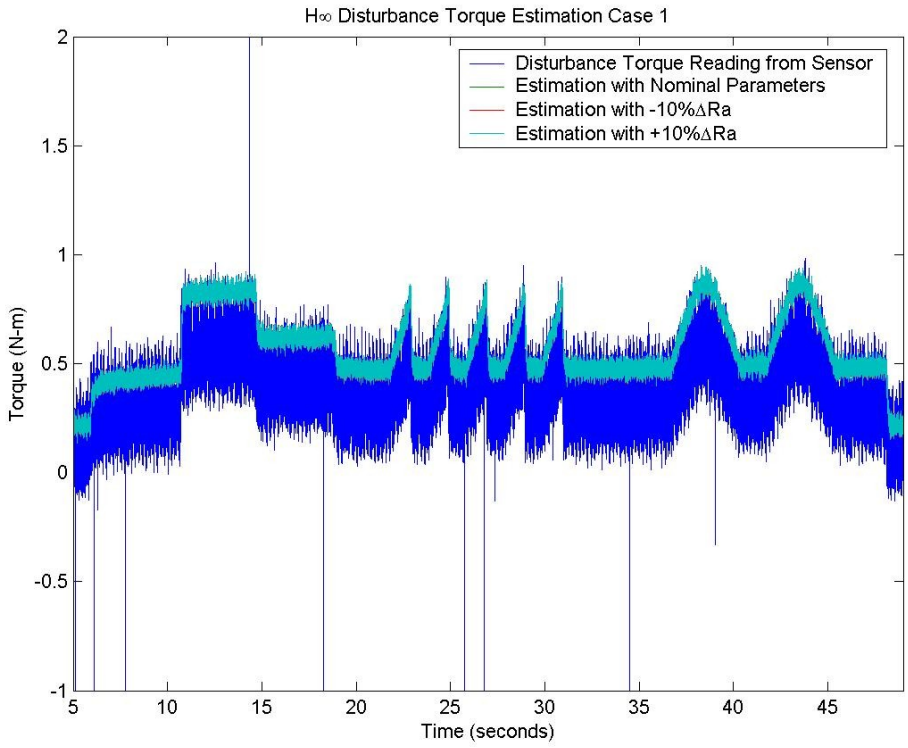

Figure 5.3 Test results for $\mathcal{H}_\infty$ disturbance torque estimation case 1.

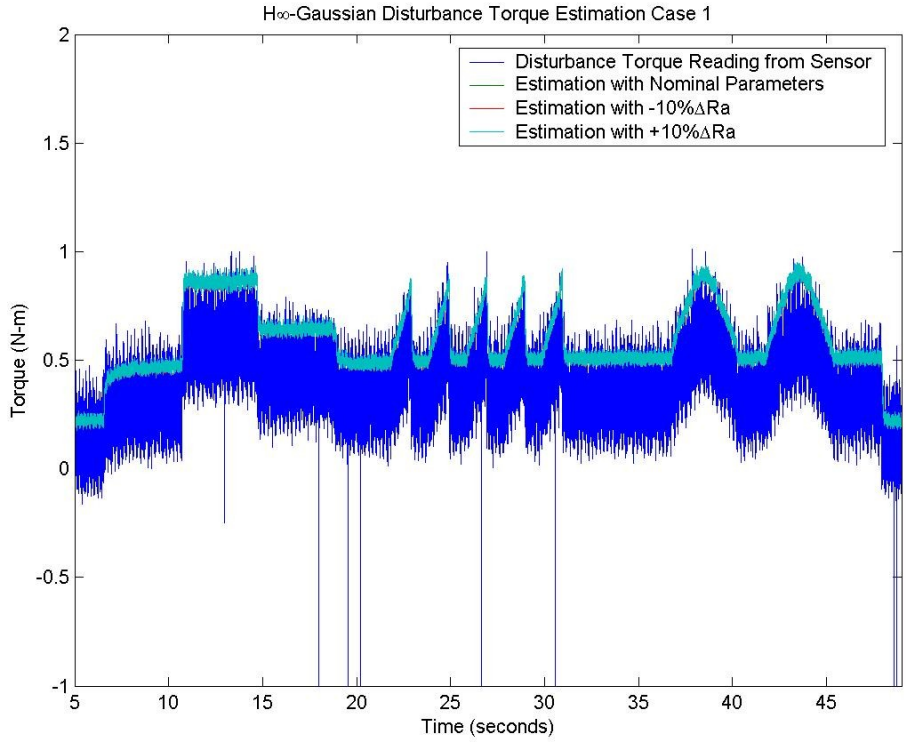

Figure 5.4 Test results for $\mathcal{H}_\infty$ Gaussian disturbance torque estimation case 1.

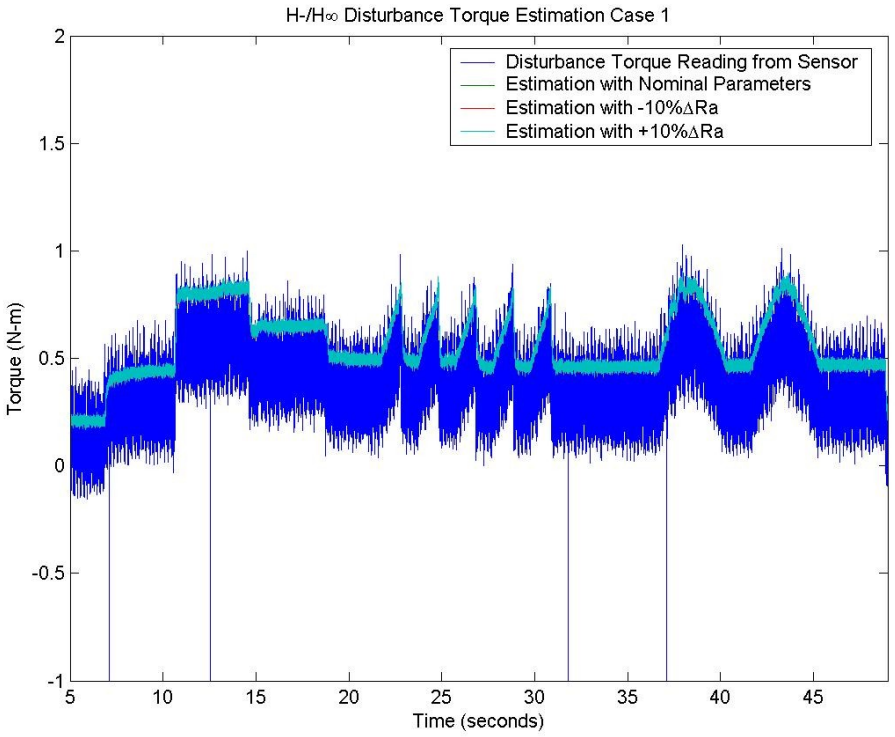

Figure 5.5 Test results for $\mathcal{H}_-/\mathcal{H}_\infty$ disturbance torque estimation case 1.

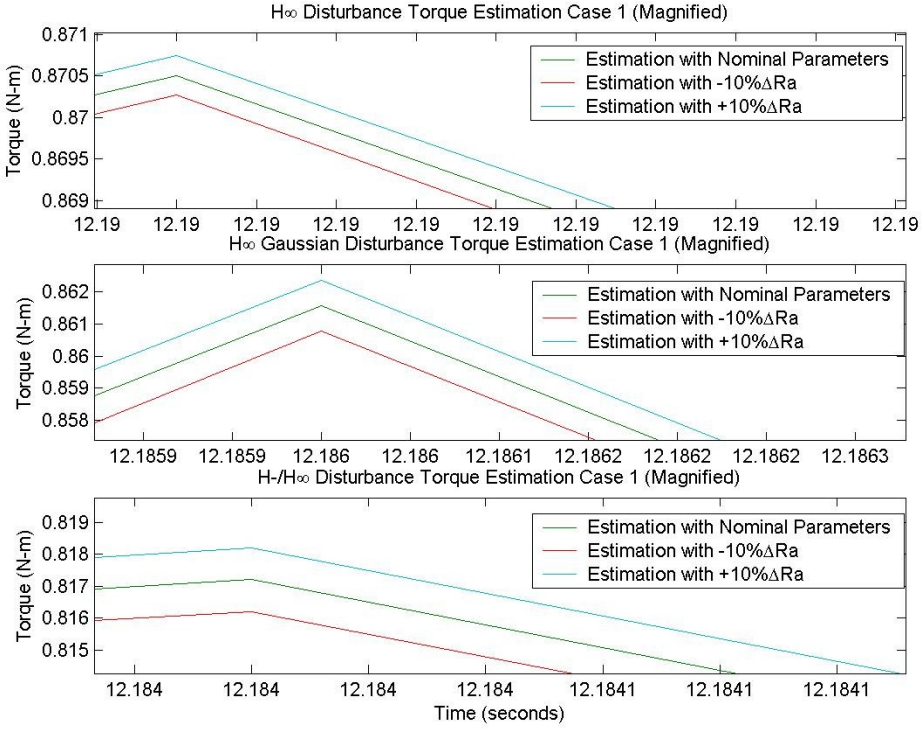

Figure 5.6 Robustness results for case 1.

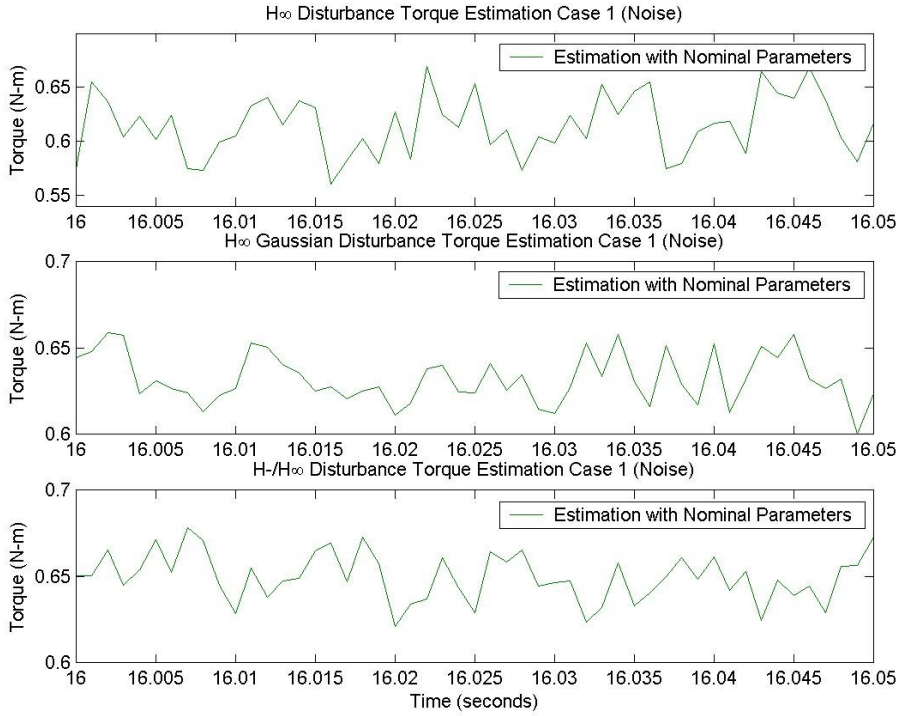

Figure 5.7 Noise results for case 1.

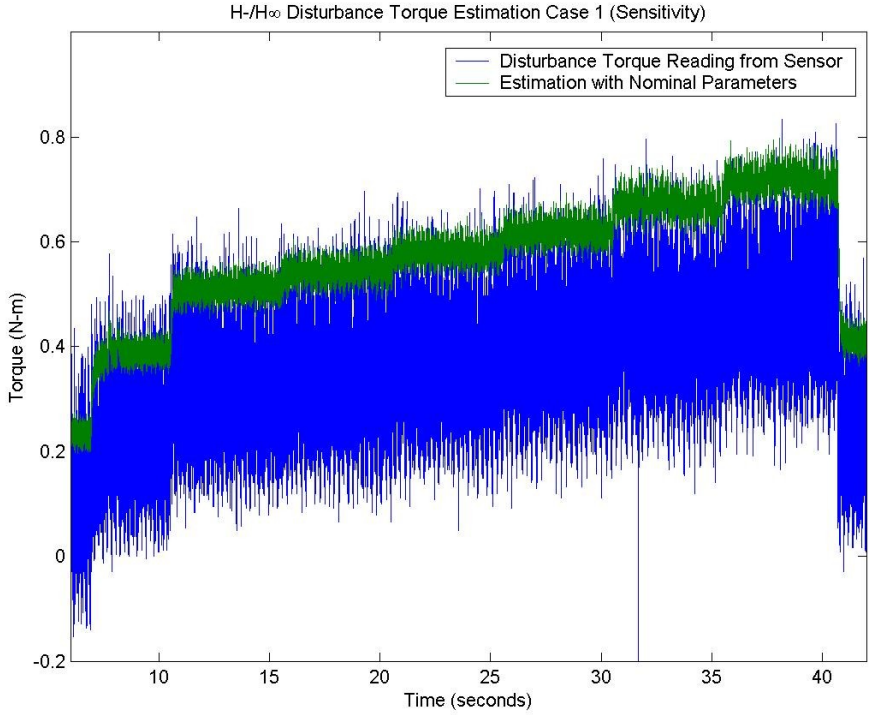

Figure 5.8 $\mathcal{H}_-/\mathcal{H}_\infty$ sensitivity results for case 1.

It can be seen in *Figure 5.3*, *Figure 5.4* and *Figure 5.5* that all of the estimators are capable of delivering appropriate and robust disturbance torque estimations in the presence of variations in the armature resistance. This is seen in the fact that the difference between all of the estimations is not even visible in the results. These results are also reinforced by *Figure 5.6* which shows that there are very small and negligible variations in the results due to the variations.

It can also be seen in *Figure 5.7* that the estimation result of the $\mathcal{H}_\infty$ Gaussian filter contains less noise in comparison to the $\mathcal{H}_\infty$ filter and $\mathcal{H}_-/\mathcal{H}_\infty$ filter estimation results. This is expected since the $\mathcal{H}_\infty$ Gaussian filter is designed to make a trade-off between robustness and noise rejection.

In *Figure 5.8* it can be clearly seen that the $\mathcal{H}_-/\mathcal{H}_\infty$ filter estimation is very sensitive to small changes in the disturbance torque. Once again this is expected since the $\mathcal{H}_-/\mathcal{H}_\infty$ filter is designed to be sensitive to the disturbance torque. This level of sensitivity may also be achieved using either the $\mathcal{H}_\infty$ filter or the $\mathcal{H}_\infty$ Gaussian filter depending on the system but is not guaranteed and would be coincidental and unique to the particular system.

5.4.2 Disturbance Torque Estimation Test Results for Case 2

For case 2, the tests were executed using nominal parameters and in the presence of variations in the electrical constant of ±10%. The first input pattern was used to generate the disturbance torque. The results for the $\mathcal{H}_\infty$, $\mathcal{H}_\infty$ Gaussian and $\mathcal{H}_-/\mathcal{H}_\infty$ disturbance torque estimations are shown in *Figure 5.9*, *Figure 5.10* and *Figure 5.11* respectively. These results were also magnified to show the robustness and noise rejection capabilities of the designed estimators and are shown in *Figure 5.12* and *Figure 5.13* respectively. Note that the noise rejection results are shown only for the estimation

with nominal parameters for the purpose of clarity. Similar results appear in the presence of uncertainties.

The second input pattern was used to test the sensitivity requirement of the $\mathcal{H}_-/\mathcal{H}_\infty$ disturbance torque estimator. The results are shown in *Figure 5.14*. Once again note that the sensitivity results are shown only for the estimation with nominal parameters for the purpose of clarity. Similar results appear in the presence of uncertainties.

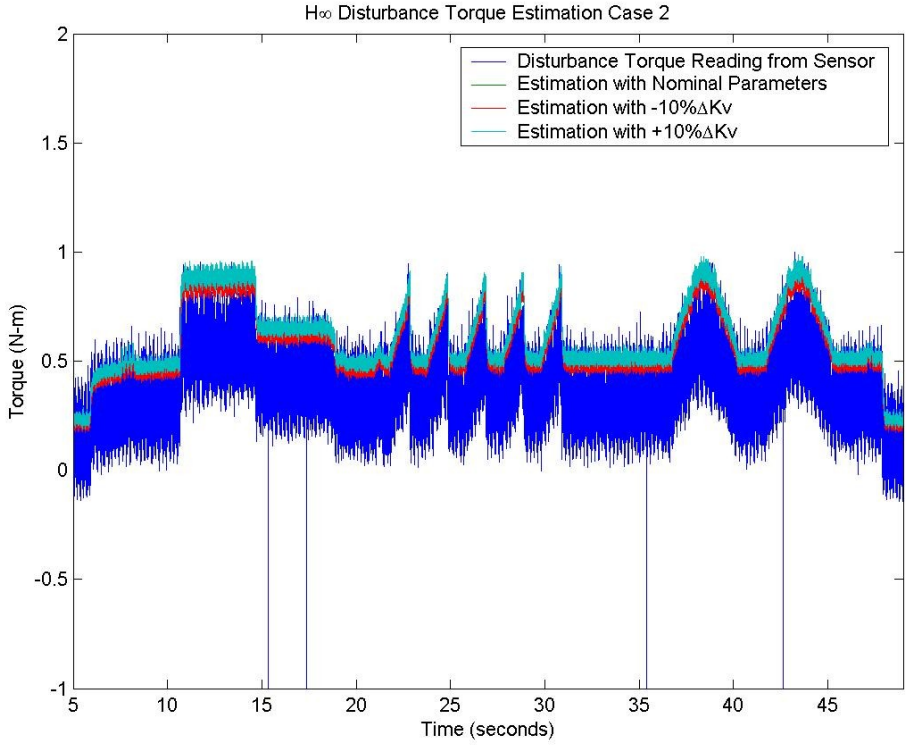

Figure 5.9 Test results for $\mathcal{H}_\infty$ disturbance torque estimation case 2.

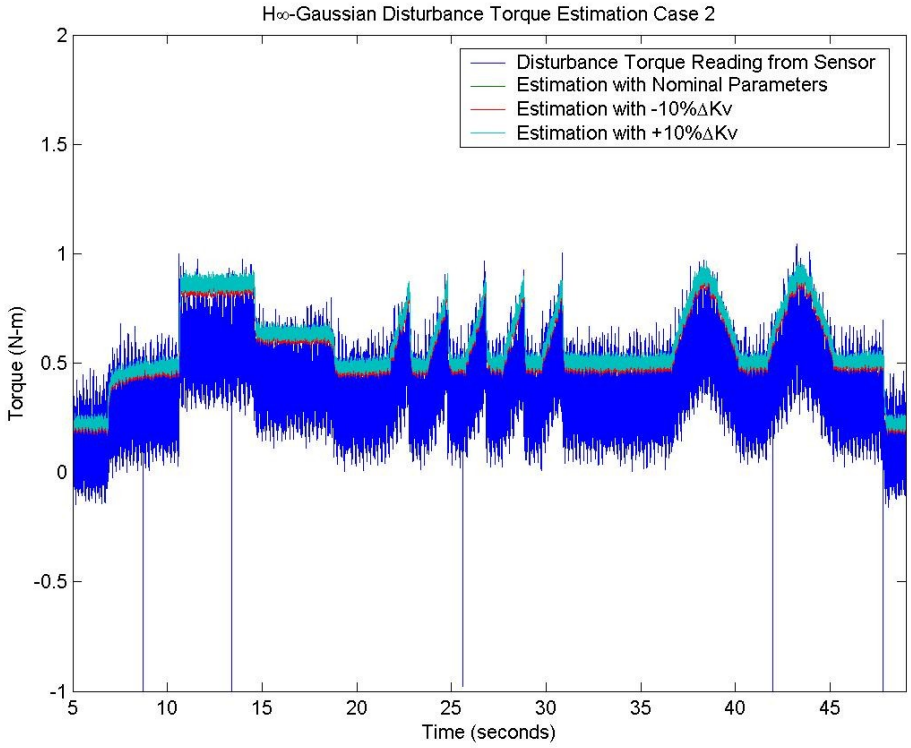

Figure 5.10 Test results for $\mathcal{H}_\infty$ Gaussian disturbance torque estimation case 2.

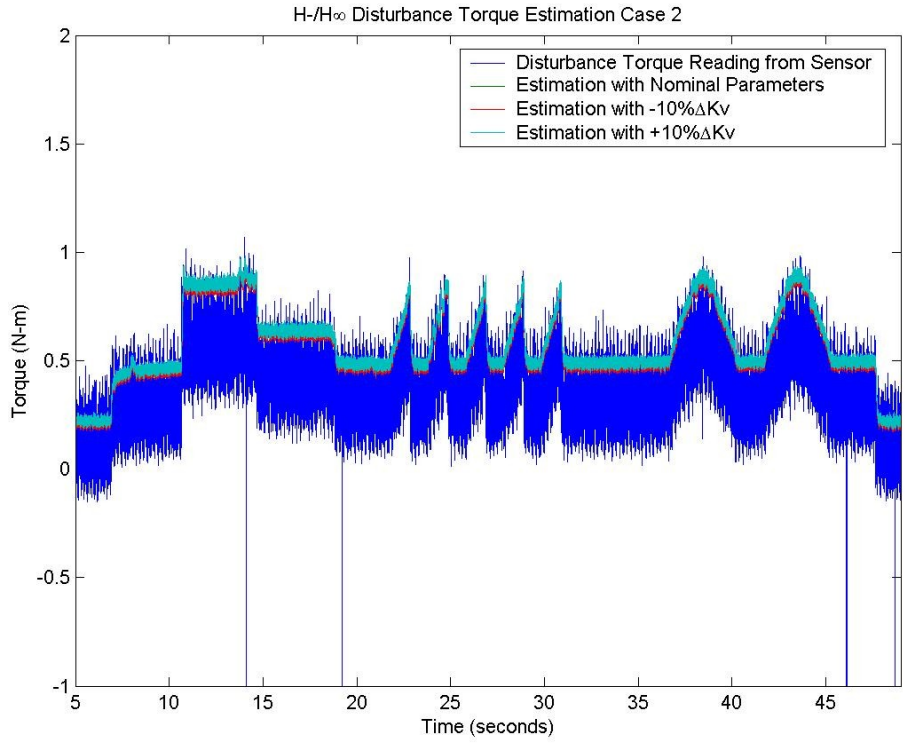

Figure 5.11 Test results for $\mathcal{H}_-/\mathcal{H}_\infty$ disturbance torque estimation case 2.

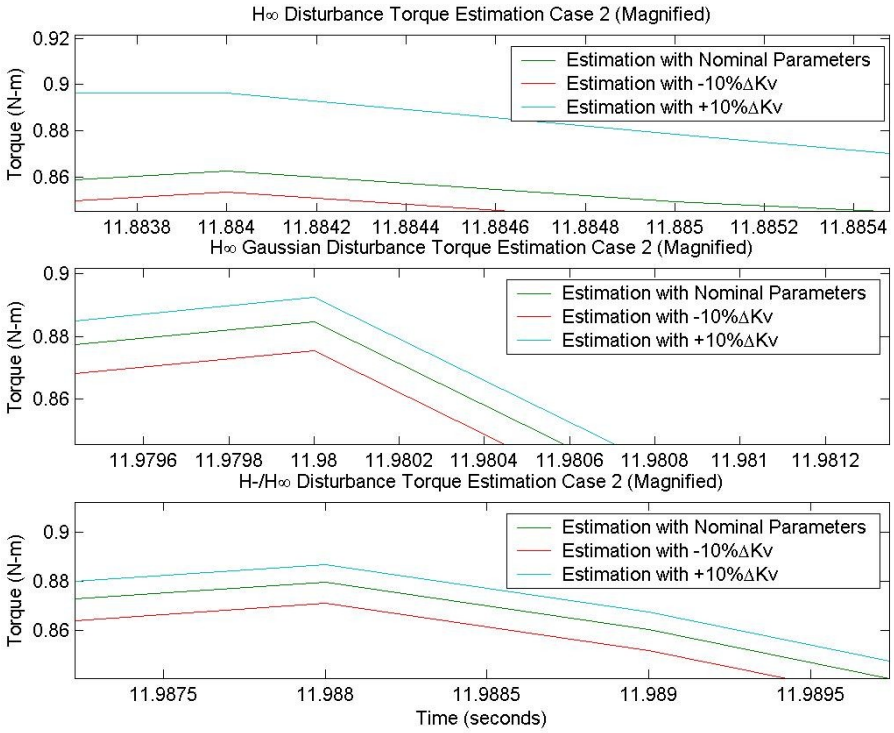

Figure 5.12 Robustness results for case 2.

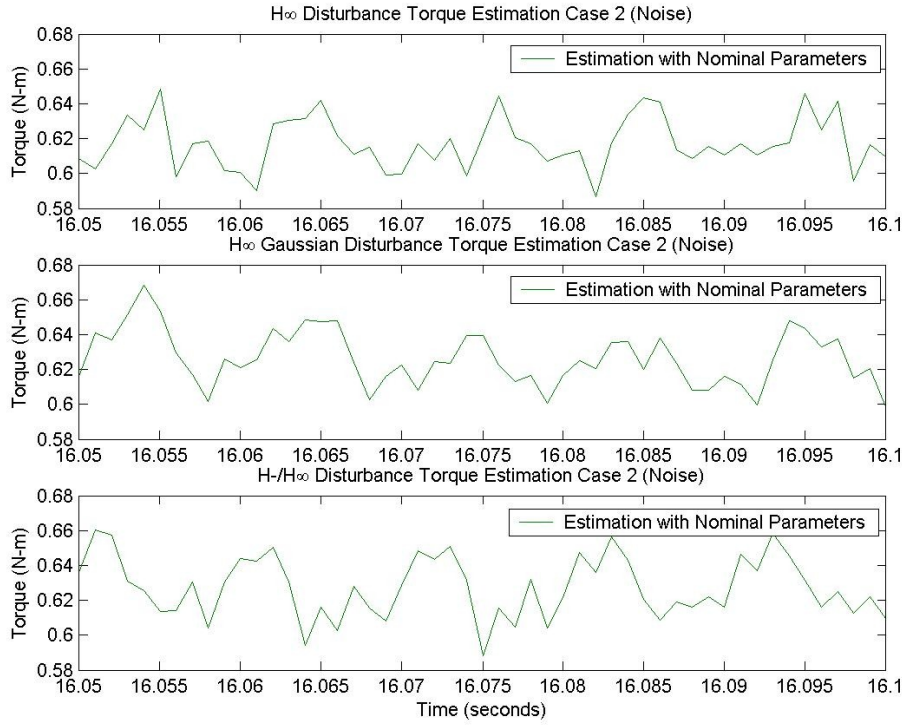

Figure 5.13 Noise results for case 2.

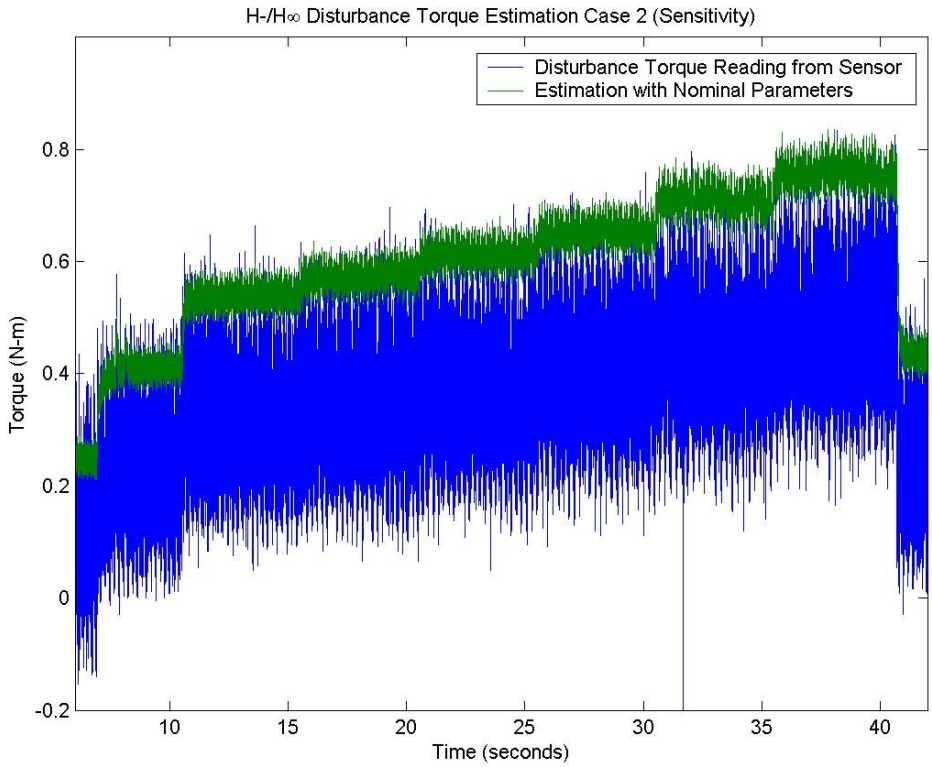

Figure 5.14 $\mathcal{H}_-/\mathcal{H}_\infty$ sensitivity results for case 2.

It can be seen in *Figure 5.9*, *Figure 5.10* and *Figure 5.11* that all of the estimators are capable of delivering appropriate and robust disturbance torque estimations in the presence of variations in the electrical constant. This is seen in the fact that the difference between all of the estimations is not even visible in the results. These results are also reinforced by *Figure 5.12* which shows that there are very small and negligible variations in the results due to the variations.

It can also be seen in *Figure 5.13* that the estimation result of the $\mathcal{H}_\infty$ Gaussian filter contains less noise in comparison to the $\mathcal{H}_\infty$ filter and $\mathcal{H}_-/\mathcal{H}_\infty$ filter estimation results as expected.

In *Figure 5.14* it can be clearly seen that the $\mathcal{H}_-/\mathcal{H}_\infty$ filter estimation is very sensitive to small changes in the disturbance torque. This is once again as expected.

This level of sensitivity may also be achieved using either the $\mathcal{H}_\infty$ filter or the $\mathcal{H}_\infty$ Gaussian filter depending on the system but is not guaranteed and would be coincidental and unique to the particular system.

5.4.3 Disturbance Torque Estimation Test Results for Case 3

For case 3, the tests were executed using nominal parameters and in the presence of variations in the armature resistance of ±10% and in the electrical constant of ±10%. The first input pattern was used to generate the disturbance torque. The results for the $\mathcal{H}_\infty$, $\mathcal{H}_\infty$ Gaussian and $\mathcal{H}_-/\mathcal{H}_\infty$ disturbance torque estimations are shown in *Figure 5.15*, *Figure 5.16* and *Figure 5.17* respectively. These results were also magnified to show the robustness and noise rejection capabilities of the designed estimators and are shown in *Figure 5.18* and *Figure 5.19* respectively. Note that the noise rejection results are shown only for the estimation with nominal parameters for the purpose of clarity. Similar results appear in the presence of uncertainties.

The second input pattern was used to test the sensitivity requirement of the $\mathcal{H}_-/\mathcal{H}_\infty$ disturbance torque estimator. The results are shown in *Figure 5.20*. Once again note that the sensitivity results are shown only for the estimation with nominal parameters for the purpose of clarity. Similar results appear in the presence of uncertainties.

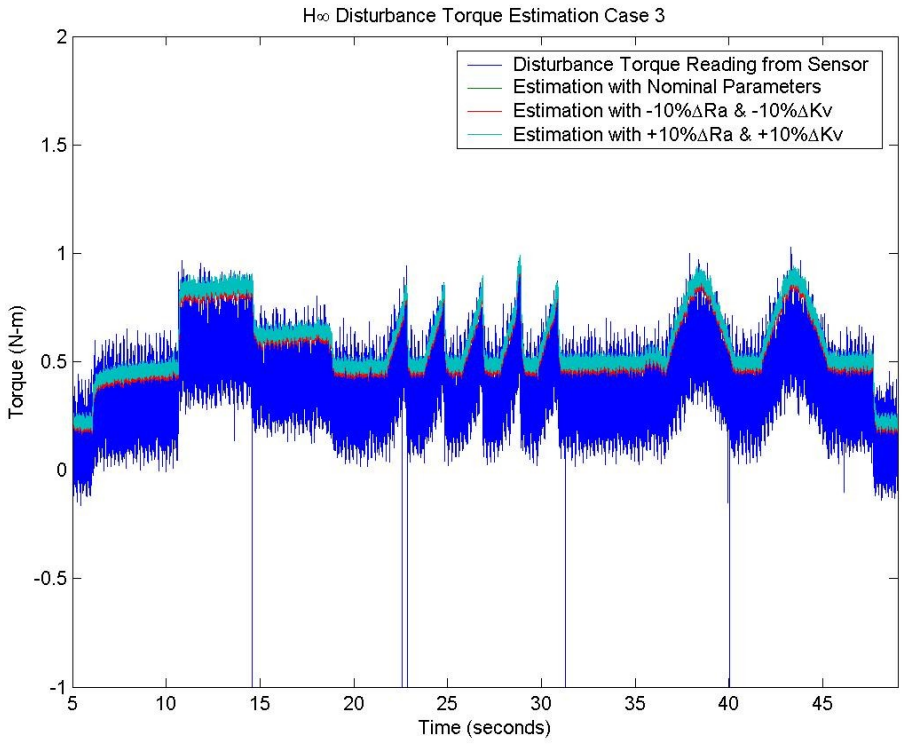

Figure 5.15 Test results for $\mathcal{H}_\infty$ disturbance torque estimation case 3.

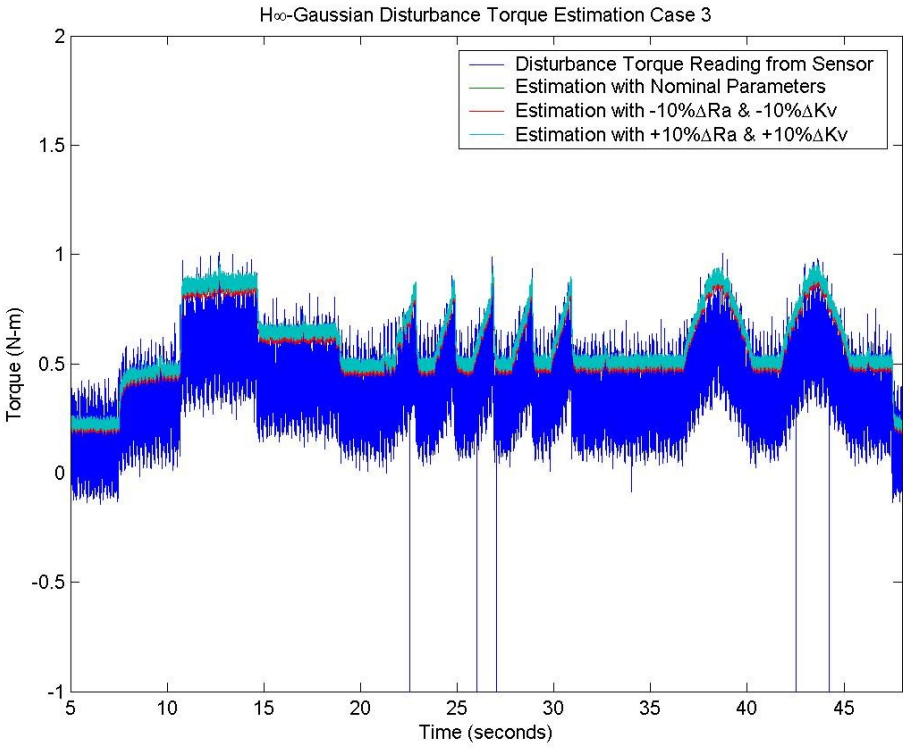

Figure 5.16 Test results for $\mathcal{H}_\infty$ Gaussian disturbance torque estimation case 3.

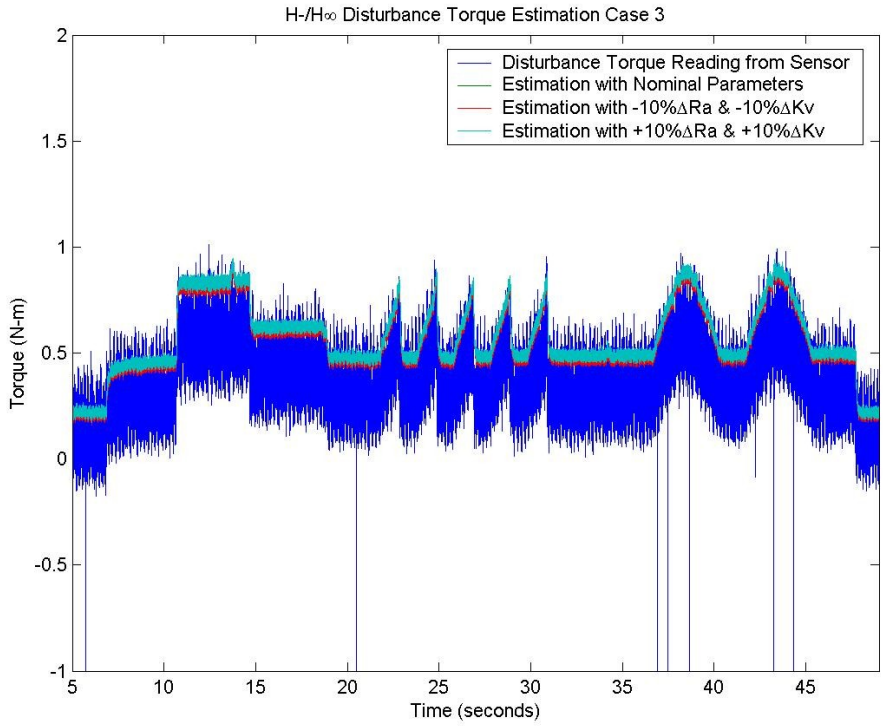

Figure 5.17 Test results for $\mathcal{H}_-/\mathcal{H}_\infty$ disturbance torque estimation case 3.

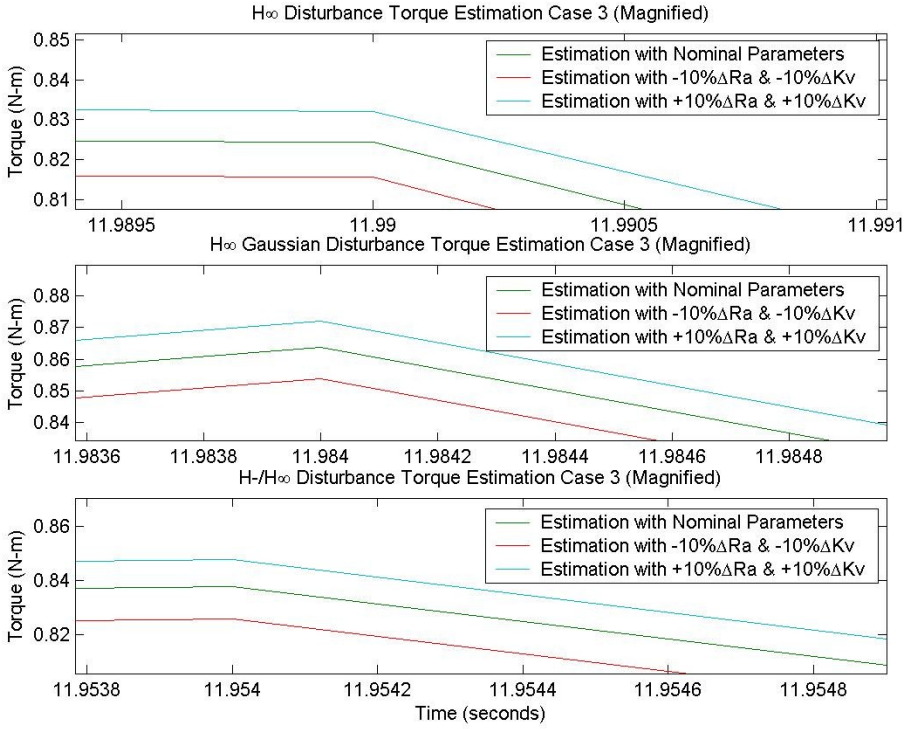

Figure 5.18 Robustness results for case 3.

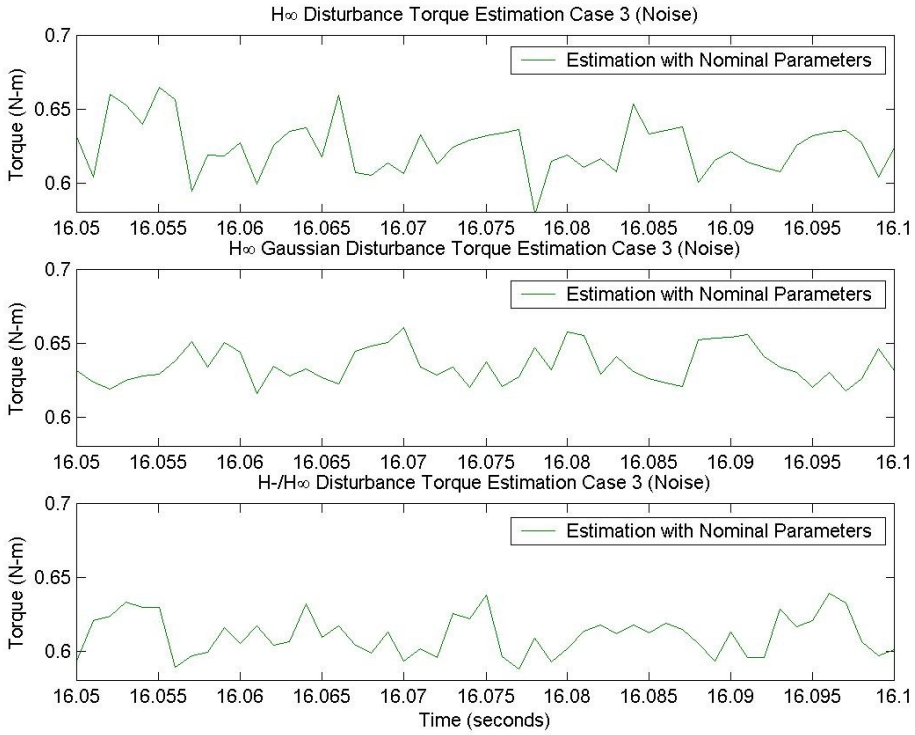

Figure 5.19 Noise results for case 3.

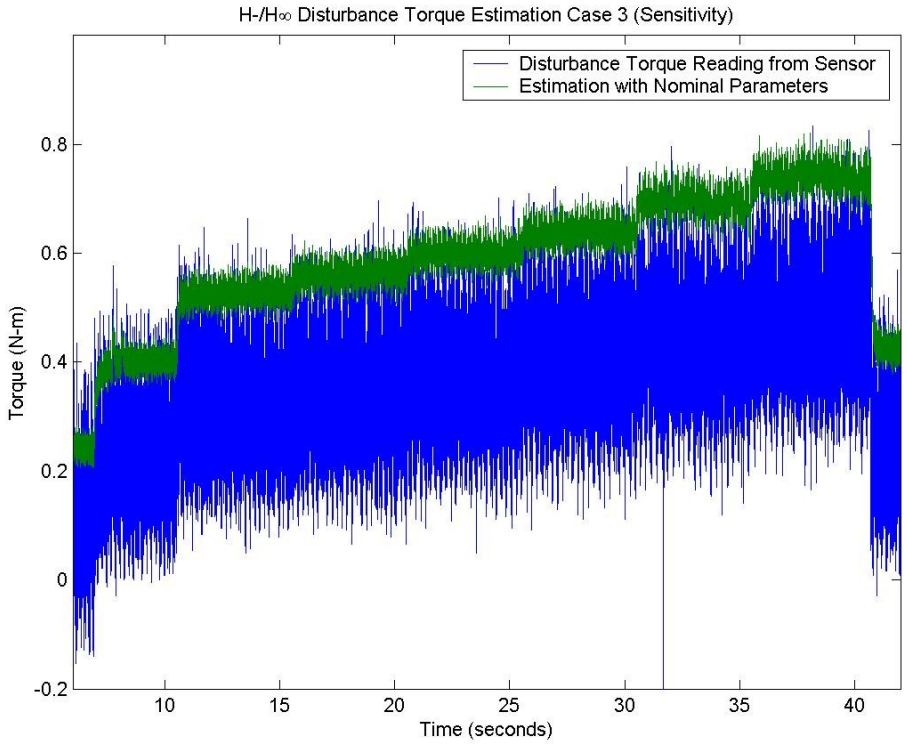

Figure 5.20 $\mathcal{H}_-/\mathcal{H}_\infty$ sensitivity results for case 3.

It can be seen in *Figure 5.15*, *Figure 5.16* and *Figure 5.17* that all of the estimators are capable of delivering appropriate and robust disturbance torque estimations in the presence of variations in both the armature resistance and the electrical constant. This is seen in the fact that the difference between all of the estimations is not even visible in the results. These results are also reinforced by *Figure 5.18* which shows that there are very small and negligible variations in the results due to the variations.

It can also be seen in *Figure 5.19* that the estimation result of the $\mathcal{H}_\infty$ Gaussian filter contains less noise in comparison to the $\mathcal{H}_\infty$ filter and $\mathcal{H}_-/\mathcal{H}_\infty$ filter estimation results as expected.

In *Figure 5.20* it can be clearly seen that the $\mathcal{H}_-/\mathcal{H}_\infty$ filter estimation is very sensitive to small changes in the disturbance torque. This is once again as expected. This level of sensitivity may also be achieved using either the $\mathcal{H}_\infty$ filter or the $\mathcal{H}_\infty$ Gaussian filter depending on the system but is not guaranteed and would be coincidental and unique to the particular system.

CHAPTER 6: CONCLUSION AND FUTURE WORK

6.1 Conclusion

DC motors can be found in many applications and have become commonplace in today's society. Their flexibility allows them to be found not only in specialized high-performance applications, but also in regular everyday applications for enhanced luxury, comfort and entertainment. As a result of this, research into both the design and control of the DC motor has been and will continue to be of great importance.

These motors unfortunately can be plagued by many factors that can inhibit their performance. The disturbance torque acting on a motor shaft can have particularly large negative effects. Knowledge of this disturbance torque can be used to mitigate the degradation in performance but direct measurement of the disturbance torque can be costly and difficult. To overcome this, estimation strategies can be used in order to obtain knowledge of the disturbance torque.

This thesis has examined the use of three robust filtering techniques to design and test three disturbance torque estimators. These include the $\mathcal{H}_\infty$ filter, the $\mathcal{H}_\infty$ Gaussian filter and the $\mathcal{H}_-/\mathcal{H}_\infty$ filter. The $\mathcal{H}_-/\mathcal{H}_\infty$ filter in particular was originally designed for use in fault detection applications and is a new a novel approach to disturbance torque estimation.

Depending upon the application, it may be necessary to ensure that the disturbance torque estimator is not only robust to model uncertainty, but that is also capable of rejecting white noise. If model uncertainty is the only factor of concern, an $\mathcal{H}_\infty$ filter based disturbance torque estimator can be designed. If both robustness and noise rejection are required, an $\mathcal{H}_\infty$ Gaussian filter based disturbance torque estimator can be designed.

Each of these designs, though, does not factor in the sensitivity to a disturbance. Examination of the error dynamics for each observer showed that the estimation error is subject not only to uncertainties, and in some cases noise, but that it is also subject to disturbances. It was also shown that the estimate of the disturbance torque is directly related to the error in estimation and thus maximization of the error's sensitivity to a disturbance should be a factor in a good estimator design. As a result, under these circumstances it is best to use an $\mathcal{H}_-/\mathcal{H}_\infty$ filter based disturbance torque estimator for the design.

Examination of the error dynamics also revealed that the these designs were capable of estimating not only constant disturbance torques, but also ones that varied with time at low frequency, i.e., the dynamics of the disturbance should not be faster than the dynamics of the estimation error.

The designed estimators were implemented and tested using an RT computer connected to a PMDC. A dyno motor was used to provide various types of disturbance torques. The estimators were subjected to various types of parameter variations as well as various types of constant and low frequency disturbance torques. The estimation results were validated using an in-line torque sensor.

In all cases, each of the designed disturbance torque estimators were shown to be capable of delivering a robust estimation of both constant and low frequency disturbance torques. Testing of the filters also showed that the $\mathcal{H}_\infty$ Gaussian filter based disturbance torque estimator has better noise rejection qualities in comparison to the $\mathcal{H}_\infty$ filter and $\mathcal{H}_-/\mathcal{H}_\infty$ filter based disturbance torque estimators. This is expected since $\mathcal{H}_\infty$ Gaussian filter is designed to make a trade-off between robustness and noise rejection.

The $\mathcal{H}_-/\mathcal{H}_\infty$ filter based disturbance torque estimator was also shown to be sensitive to small changes in the disturbance torque. Once again this is expected since the $\mathcal{H}_-/\mathcal{H}_\infty$ filter is designed to be sensitive to the disturbance. This level of sensitivity may also be achieved using either the $\mathcal{H}_\infty$ filter or the $\mathcal{H}_\infty$ Gaussian filter based disturbance torque estimators but is not guaranteed. This kind of result would be coincidental and unique to the particular system and may not prove true for any other system in general.

6.2 Future Work

Continued testing should be done in order to further tune the disturbance torque estimation. This can be done by varying the degree of tolerance to uncertainty and/or noise of the observer, or by varying the significance of a particular uncertainty on the disturbance torque estimation. Each time a new set of parameters is chosen, the changes in the estimation should be noted. This could aid in not only optimization of the disturbance torque estimation but could also in the development of a systematic method to tune the estimation parameters.

Reduction of observer order and its effects on the disturbance torque estimation should also be investigated. This could lead to the development of a reduced order observer design for the disturbance torque estimator. The benefit of such a design would be the reduction in resources required to implement such an estimation algorithm as opposed to a full order observer based estimation algorithm. This reduction in resources could also lead to a reduction in overall system cost.

The $\mathcal{H}_-/\mathcal{H}_\infty$ filter design technique has been shown to work as a basis for a disturbance torque estimator design when applied to a PMDC system. Generalization of this type of design should be studied in order show that such an estimation scheme is

not restricted solely to a PMDC system, but that it can also be applied to a wide variety of other systems.

Since the ultimate goal of developing a disturbance torque estimation scheme is to compensate for the effects of the disturbance torque acting on the system, methods on how to use the estimation for control should be examined. One possibility would be to use model recovery techniques to acquire a mathematical model of the disturbance torque from the estimation as opposed to instantaneous values of the disturbance torque generated by the estimation algorithms at each sampling interval when implemented in a digital system. The model of the disturbance torque could be updated at regular intervals of time and the controller made to adapt to these changes based on the internal model principle.

REFERENCES

[1] G. S. Buja, R. Menis, and M. I. Valla, “Disturbance Torque Estimation in a Sensorless DC Drive,” *IEEE Transactions on Industrial Electronics*, vol. 42, no. 4, pp. 351–357, 1995.

[2] R. C. Dorf and R. H. Bishop, *Modern Control Systems*, 11th ed. Upper Saddle River, New Jersey, USA: Pearson Education Inc., 2008.

[3] G. F. Franklin, J. D. Powell, and A. Emami-Naeini, *Feedback Control of Dynamic Systems*, 4th ed. Upper Saddle River, New Jersey, USA: Prentice-Hall, Inc., 2002.

[4] D. G. Luenberger, “Observing the State of a Linear System,” *IEEE Transactions on Military Electronics*, vol. MIL-8, pp. 74–80, 1964.

[5] D. G. Luenberger, “An Introduction to Observers,” *IEEE Transactions on Automatic Control*, vol. AC-16, no. 6, pp. 596–602, 1971.

[6] M. Lawson and X. Chen, “Fault Tolerant Control for an Electric Power Steering System,” in *IEEE International Conference on Control Applications*, 2008, pp. 486–491.

[7] M. Lawson and X. Chen, “Hardware-in-the-Loop Simulation of Fault Tolerant Control for an Electric Power Steering System,” in *IEEE Vehicle Power and Propulsion Conference*, 2008, pp. 1–6.

[8] W. S. Levine, Ed., *The Control Handbook*. Boca Raton, Florida, USA: CRC Press, INC., 1999.

[9] D. Simon, *Optimal State Estimation: Kalman, H-infinity, and Nonlinear Approaches*. Hoboken, New Jersey, USA: John Wiley & Sons, Inc., 2006.

[10] K. Zhou and J. C. Doyle, *Essentials of Robust Control*. Upper Saddle River, New Jersey, USA: Prentice-Hall, Inc., 1998.

[11] X. Chen and K. Zhou, "Multiobjective $\mathcal{H}_2/\mathcal{H}_\infty$ Control Design," *SIAM J. Control Optim*., vol. 40, no. 2, pp. 628–660, 2001.

[12] X. Chen and K. Zhou, "$\mathcal{H}_\infty$ Gaussian Filter on Infinite Time Horizon," *IEEE Transactions on Circuits and Systems-I: Fundamental Theory and Applications*, vol. 49, no. 5, pp. 674–679, 2002.

[13] Y. Choi, K. Yang, W. K. Chung, H. R. Kim, and I. H. Suh, "On the Robustness and Performance of Disturbance Observers for Second-Order Systems," *IEEE Transactions on Automatic Control*, vol. 48, no. 2, pp. 315–320, 2003.

[14] K. Fujiyama, M. Tomizuka, and R. Katayama, "Digital Tracking Controller Design for CD Player Using Disturbance Observer," in *AMC'98 - Coimbra. 1998 5th International Workshop on Advanced Motion Control. Proceedings*, 1998, pp. 598–603.

[15] Y. I. Son, H. Shim, N. H. Jo, and S.-J. Kim, "Design of Disturbance Observer for Non-Minimum Phase Systems Using PID Controllers," in *SICE Annual Conference* 2007, 2007, pp. 196–201.

[16] C.-C. Wang and M. Tomizuka, "Design of Robustly Stable Disturbance Observers Based on Closed Loop Consideration Using $\mathcal{H}_\infty$ Optimization and its Applications to Motion Control Systems," in *Proceedings of the 2004 American Control Conference*, 2004, pp. 3764–3769.

[17] M. Hou and R. J. Patton, "An LMI Approach to $\mathcal{H}_-/\mathcal{H}_\infty$ Fault Detection Observers," in *UKACC International Conference on CONTROL*, 1996, pp. 305–310.

[18] X. Li and K. Zhou, “A Time Domain Approach to Robust Fault Detection of Linear Time-Varying Systems,” in *Proceedings of the 46th IEEE Conference on Decision and Control*, 2007, pp. 1015–1020.

[19] X. Li and K. Zhou, “Fault Detection for Linear Discrete-Time Invariant Systems with Decoupling and Optimization,” in *Joint 48th IEEE Conference on Decision and Control and 28th Chinese Control Conference*, 2009, pp. 990–995.

[20] X. Li and K. Zhou, “A Time Domain Approach to Robust Fault Detection of Linear Time-Varying Systems,” *Automatica*, vol. 45, no. 1, pp. 94–102, 2009.

[21] N. Liu and K. Zhou, “Optimal Solutions to Multi-Objective Robust Fault Detection Problems,” in *Proceedings of the 46th IEEE Conference on Decision and Control*, 2007, pp. 981–988.

[22] N. Liu and K. Zhou, “Optimal Robust Fault Detection for Linear Discrete Time Systems,” in *Proceedings of the 46th IEEE Conference on Decision and Control*, 2007, pp. 989–994.

[23] N. Liu and K. Zhou, “Optimal Robust Fault Detection for Linear Discrete Time Systems,” *Journal of Control Science and Engineering*, vol. 2008, no. 7, 2008.

[24] K. Zhou and Z. Ren, “ A New Controller Architecture for High Performance, Robust, and Fault-Tolerant Control,” *IEEE Transactions on Automatic Control*, vol. 46, no. 10, pp. 1613-1618, 2001.

[25] N. Mohan, T. M. Undeland, and W. P. Robbins, *Power Electronics: Converters, Applications, and Design*. John Wiley & Sons, Inc., 2003.

[26] Baldor Electric Company, *DC Motor Performance Data Record # 499*. Fort Smith, Arkansas, USA: Baldor Electric Company, 2010.

[27] Bosch, “Products Datasheet DC Motors Without Gear Assembly GPA 12 V 400 W,” [Online]. Available: http://www.boshmotorsandcontrols.co.uk/elektromotoren/produkt/0130302003/index.htm

[28] RoboteQ Inc., *AX1500 Dual Channel Digital Motor Controller User’s Manual*, v1.9b ed. USA: RoboteQ Inc., 2007, vol. v1.9b.

[29] RoboteQ Inc., *AX3500 Dual Channel High Power Digital Motor Controller User’s Manual*, v1.9b ed. USA: RoboteQ Inc., 2007, vol. v1.9b.

[30] Sensor Developments Inc., *Rotating Torque Sensor with Digital Telemetry Model: 01424 Operator’s Manual*. USA: Sensor Developments Inc., 2010.

[31] Gurley Precision Instruments, “Gurley Series 9X25 Rotary Incremental Encoders Data Sheet,” USA. [Online]. Available: http://www.gurley.com/Encoders/Info/925.pdf

[32] Opal-RT Technologies Inc., *RT-Lab 6.0 User’s Manual*. Canada: Opal-RT Technologies Inc., 2002.

VITA AUCTORIS

NAME:	Danny Grignion
PLACE OF BIRTH:	Leamington, Ontario, Canada
YEAR OF BIRTH:	1987
EDUCATION:	**Master of Applied Science (M.A.Sc.)** Electrical Engineering University of Windsor, Windsor, Ontario, Canada 2010-2012
	Bachelor of Applied Science (B.A.Sc.) Honours Electrical Engineering University of Windsor, Windsor, Ontario, Canada 2006-2010